University of Szeged

Faculty of Pharmacy

Institute of Pharmaceutical Technology and Regulatory Affairs

Head: Prof. Dr. Ildikó Csóka Ph.D.

Ph.D. Thesis

FORMULATION OF MELOXICAM POTASSIUM-CONTAINING, CYCLODEXTRIN-BASED NASAL POWDERS VIA SPRAY DRYING

dr. Patricia Orsolya Varga

Pharmacist

Supervisors:

Dr. Csilla Balla-Bartos Ph.D.

and

Prof. Dr. Rita Ambrus D.Sc.

SZEGED

2025

Publications related to the subject of the thesis

1) Patrícia Varga, Rita Ambrus, Piroska Szabó-Révész, Dávid Kókai, Katalin Burián, Zsolt Bella, Ferenc Fenyvesi, Csilla Bartos; Physico-Chemical, In Vitro and Ex Vivo Characterization of Meloxicam Potassium-Cyclodextrin Nanospheres; Pharmaceutics; Pharmaceutics; 2021, 13, 1833, DOI: 10.3390/pharmaceutics13111883, impact factor: 6.441 (2021), Q1 (2021)
2) Patrícia Varga, Csilla Bartos, Rita Ambrus; Stability testing of cyclodextrin-based meloxicam potassium containing nanospheres intended for nasal administration; Acta Pharmaceutica Hungarica; 2023, 93, 57-62, DOI: 10.33892/aph.2023.93.57-62, impact factor: -, Q4 (2023)
3) Patrícia Varga, Anett Németh, Scarlett Zeiringer, Eva Roblegg, Mária Budai-Szűcs, Csilla Balla-Bartos, Rita Ambrus; Formulation and investigation of differently charged β-cyclodextrin-based meloxicam potassium containing nasal powders; European Journal of Pharmaceutical Sciences; 2024, 202, 106879, DOI: 10.1016/j.ejps.2024.106879, impact factor: 5.147 (2024), Q1 (2024)

Publications not related to the subject of the thesis

1) Csilla Bartos, Patrícia Varga, Piroska Szabó-Révész, Rita Ambrus; Physico-chemical and in vitro characterization of chitosan-based microspheres intended for nasal administration; Pharmaceutics, 2021 13(5), 608. DOI: 10.3390/pharmaceutics13050608, impact factor: 6.4 (2021), Q1 (2021)
2) Edit Benke, Patrícia Varga, Piroska Szabó-Révész, Rita Ambrus; Stability and in vitro aerodynamic studies of inhalation powders containing ciprofloxacin hydrochloride applying different DPI capsule types; Pharmaceutics, 2021, 13(5), 689, DOI: 10.3390/pharmaceutics13050689, impact factor: 6.4 (2021), Q1 (2021)
3) Csilla Bartos, Piroska Szabó-Révész, Tamás Horváth, Patrícia Varga, Rita Ambrus; Comparison of modern in vitro permeability methods with the aim of investigation nasal dosage forms; *Pharmaceutics*, 2021, *13*(6), 846. DOI: 10.3390/pharmaceutics13060846, impact factor: 6.4 (2021), Q1 (2021)
4) Areen Alshweiat, Patrícia Varga, Ildikó Csóka, Anett Németh, Csilla Bartos, Rita Ambrus; Preparation and characterization of smartcrystals for dissolution enhancement of poorly water-soluble niflumic acid; Farmacia, 2023, 71(3). DOI: 10.31925/farmacia.2023.3.7, impact factor: 1.4, Q2 (2023)

Presentations related to this thesis

Oral presentations

1) **Varga P**., Ambrus R., Balla-Bartos Cs.: Nazális bevitel céljából előállított meloxikám-kálium tartalmú nanoszférák vizsgálata, MKE Kristályosítási és Gyógyszerformulálási Szakosztály 13. Kerekasztal Konferenciája (2021)
2) **Varga P**., Németh A.: Különböző töltéssel rendelkező β-ciklodextrin alapú meloxikám-kálium-tartalmú nazális porok vizsgálata, XV. Clauder Ottó Emlékverseny (2023)
3) **Varga P**., Balla-Bartos Cs., Ambrus R.: Meloxikám-kálium tartalmú nazális porok stabilitásvizsgálata, XXVI. Tavaszi Szél Konferencia, Pécs (2023)
4) **Varga P**., Németh A., Budai-Szűcs M., Balla-Bartos Cs., Ambrus R.: Evaluation of different β-cyclodextrins- and polymer-containing nasal powders, VI. Symposium of Young Researchers on PharmaceuticalTechnology, Biotechnology and Regulatory Science, Szeged (2024)
5) Ambrus R., **Varga P**., Németh A., Balla-Bartos Cs., Csóka I.: Application of Cyclodextrins in Traditional and Alternative Drug Formulations; Case Studies, Conference on Pharmacology, Pharmacokinetics & Innovation (HUPHAR 2024), Mátraháza (2024)

Poster presentations

1) **Varga P**., Balla-Bartos Cs., Ambrus R.: Investigation Of Meloxicam Potassium Containing Nanoparticles For Intranasal Administration, 9th BBBB International Conference on Pharmaceutical Sciences, Ljubljana (2022)
2) Motzwickler-Németh A., **Varga P**., Budai-Szűcs M., Csóka I. Investigation of the nasal applicability of different charged cyclodextrin-based meloxicam potassium containing particles, EUROCD 2023 7th European Cyclodextrin Conference, Budapest (2023)
3) **Varga P**., Balla-Bartos Cs., Ambrus R.: Stability testing ofcyclodextrin-based meloxicam potassium containing nasal powders, EUROCD 2023 7th European Cyclodextrin Conference, Budapest (2023)
4) **Varga P**., Balla-Bartos Cs., Ambrus R.: Accelerated stability study of differently charged β-cyclodextrin-PVA based nasal powders, Congressus Pharmaceuticus Hungaricus XVII. and EUFEPS Annual Meeting 2024, Debrecen (2024)

Abbreviations

API	Active pharmaceutical ingredient
ALI	Air-liquid interface
BCD	β-cyclodextrin
CD	Cyclodextrin
CNS	Central nervous system
COX	Cyclooxygenase
DSC	Differential scanning calorimetry
FT-IR	Fourier transform infrared spectroscopy
HA	Sodium hyaluronate
HPBCD	Hydroxypropyl β-cyclodextrin
HPLC	High performance liquid chromatography
HPMC	Hydroxypropyl methyl cellulose
ICH	International Council for Harmonisation of Technical Requirements for Pharmaceuticals for Human Use
LDH	Lactate dehydrogenase
MTS	3-(4,5-dimethylthiazol-2-yl)-5-(3-carboxymethoxyphenyl)-2-(4-sulfophenyl)-2H-tetrazolium
MXP	Meloxicam potassium
NSAID	Non-steroidal anti-inflammatory drug
PBS	Phosphate buffer
PM	Physical mixture
PVA	Polyvinyl alcohol
QABCD	Quaternary ammonium β-cyclodextrin

SBECD	Sulfobutylether β-cyclodextrin sodium salt
SD	Spray-dried
SEM	Scanning electron microscopy
SNES	Simulated nasal electrolyte solution
XRPD	X-ray powder diffractometry

TABLE OF CONTENTS

1. INTRODUCTION 1
2. AIM OF THE WORK 2
3. LITERATURE BACKGROUND OF THE RESEARCH WORK 4
3.1 Nose as an alternative drug delivery route 4
3.2 Excipients in nasal drug delivery 7
3.2.1. Cyclodextrins 7
3.2.2. Polymers 9
3.3 Nasal dosage forms – powders 11
3.4 Pain management – nasal alternatives 14
4. MATERIALS AND METHODS 17
4.1. Materials 17
4.1.1. Active pharmaceutical ingredient (API) 17
4.1.2. Excipients 17
4.2. Methods 19
4.2.1. Preparation method of the spray-dried samples 19
4.2.2. Physico-chemical characterization 20
4.2.3. In vitro measurements 21
4.2.4. Accelerated stability test of the selected samples 23
4.2.5. Cell-based measurements 23
4.2.6. MXP-content determination by high performance liquid chromatography (HPLC) 25
5. RESULTS AND DISCUSSION 26
5.1. Physico-chemical characterization of the prepared samples 26
5.1.1. Particle size and morphology of the spray-dried samples 26
5.1.2. Crystallinity of the samples 27
5.1.3. Thermal behavior of the samples 28
5.1.4. Secondary interactions in the formulations 30
5.2 *In vitro* measurements 31
5.2.1. In vitro mucoadhesion test 31
5.2.2 In vitro dissolution of MXP from the samples 33
5.2.3 In vitro permeation studies applying an artificial mucosa 34
5.3. Accelerated stability testing of the selected samples 36
5.3.1. Morphology of the spray-dried particles 36
5.3.2. Physico-chemical stability of the samples 37
5.3.3. Drug content change in the samples 38

5.3.4. Short discussion on the stability results 39
5.4. Cell-based measurements 39
5.4.1. In vitro toxicity on RPMI 2650 cells 39
5.4.2. In vitro permeation studies applying RPMI 2650 nasal cells 41
6. CONCLUSIONS 43

1. INTRODUCTION

Nasal drug delivery has become a promising non-invasive route due to its high vascularization, rapid onset of action, and potential for avoiding first-pass metabolism. This route can facilitate direct drug delivery to the systemic circulation enhancing therapeutic efficacy [1]. However, the nasal route faces challenges such as the inefficient permeation of drugs through the nasal mucosa and the rapid clearance of the formulations from the nasal cavity due to the mucociliary clearance [2]. These challenges necessitate innovative strategies to enhance drug absorption and prolong the residence time of nasal formulations.

Cyclodextrins have gained considerable attention in the pharmaceutical industry. Their ability to form inclusion complexes with a variety of drugs enhances solubility and stability, resulting in improved permeation [3]. Additionally, they can interact with biological membranes disrupting the cell membrane fluidity and the tight junctions between epithelial cells, enhancing the drug molecules' permeation through the mucosa [4].

While cyclodextrins enhance permeation, the rapid clearance of formulations from the nasal cavity remains a significant challenge. To address this, the incorporation of water-soluble polymers was explored [5]. These polymers can increase the viscosity of the formulation, thereby prolonging the residence time in the nasal cavity.

Nasal powders produced by spray drying may also provide prolonged residence time in the nasal cavity compared to liquid formulations due to their better adhesion, thus reduced mucociliary removal [6]. Furthermore, preservatives are unnecessary in the formulation process, and the fine particle size achieved through spray drying ensures optimal deposition and absorption of the drug within the nasal cavity.

Nasal systemic delivery of non-steroidal anti-inflammatory drugs (NSAIDs) is a less explored area; however, they could serve as quick pain relievers or could be adjuncts to opioid therapy.

To the best of our knowledge, no study is available in the literature, where spray-dried cyclodextrin-based nasal powders are investigated in combination with water-soluble polymers in order to deliver an NSAID to the systemic circulation through the nasal route. This Ph.D. work aims to study the applicability of different cyclodextrins in combination with water-soluble polymers with a purpose to contribute to the advancement of solid nasal drug delivery systems.

2. AIM OF THE WORK

This PhD work aimed to produce solid nasal dosage forms containing an NSAID, meloxicam potassium (MXP) monohydrate with different excipients. The following steps were planned to conduct during our work:

I. An extensive review of the literature was proposed to determine the key characteristics of solid nasal dosage forms, their preparation techniques and the requirements of the applicable excipients.

II. After studying the literature, nano spray drying was chosen as the preparation method with the aim of preparing particles with a diameter of <5 μm. An essential physico-chemical characterization of the prepared formulations was planned to carry out. The particle size and morphology, crystallinity, thermal behavior of the samples and the potentially formed secondary interactions were aimed to be observed to reveal the effect of the preparation procedure on the properties of the powders.

III. The *in vitro* properties, like mucoadhesion, dissolution and permeation rate of the samples were planned to study to observe the effect of the applied excipients and to choose the best-performing formulations for further stability and cell culture measurements.

IV. Our aim was also to screen the selected formulations with accelerated stability tests according to the International Council for Harmonization (ICH) Q1A guideline. The results of the stability test together with the *in vitro* measurements were intended to be the basis of the sample selection for further nasally relevant cell culture measurements.

V. Besides, our goal was to determine the non-toxic concentrations of the applied cyclodextrins and raw MXP. Furthermore, the non-toxic concentrations of the selected formulations were intended to be evaluated to be able to proceed with the permeation studies safely.

VI. Applying RPMI 2650 cells, the MXP permeation from the raw API and the selected formulations were planned to be examined to observe if the cyclodextrins had any permeation enhancing effect.

VII. Lastly, the effect of the incorporated excipients – different cyclodextrins and water-soluble polymers – on the properties of the formulations and on their nasal applicability were intended to be evaluated.

Despite the significant role that cyclodextrins play in the pharmaceutical industry, their application in nasal delivery systems has remained less exploited. Furthermore, there is a need for research to provide patients with more options for nasal pain reliving by NSAIDs. Thus, the primary objective of this Ph.D. work was to contribute to the development of future nasal powder products by collecting novel results on such formulations containing MXP, water-soluble polymers and cyclodextrins.

3. LITERATURE BACKGROUND OF THE RESEARCH WORK

3.1 Nose as an alternative drug delivery route

Most of the active pharmaceutical ingredients (APIs) are administered *per os* or intravenously, although in the former case, the enzymatic deactivation of the drugs reduces the amount that is absorbed to the circulation, in the latter case, the process comes with stress for patients and only trained workers are allowed to complete the administration [7,8]. For these reasons, it is important to find non-invasive alternative routes that can easily and effectively target the systemic circulation in the absence of qualified personnel with less inconvenience for patients. The nasal route has gained considerable attention as an alternate to the oral or parenteral delivery routes bypassing some of the major limitations due to its unique anatomical and physiological features [9,10]. Nevertheless, it has its own challenges to tackle in order of successful drug delivery [11–13].

The volume of the nasal cavity is approximately 15 mL and divided into two halves by the nasal septum [14]. It has an anterior part called the vestibule, a respiratory region and an olfactory region. The cellular composition is different in each region and accordingly, they have their own function.

The vestibule consists of stratified squamous epithelium and hair follicles serving as a protector against larger particles getting into the lungs. It is not significant in terms of drug delivery. The respiratory region is the largest section of the nasal cavity covered by pseudostratified columnar epithelium – typical airway epithelium – consisting of ciliated and non-ciliated cells as well as goblet cells [14]. Its physiological function is to warm and humidify the inspired air and it is the target of most of the nasal products [15]. The olfactory area can be found at the ceiling of the cavity, and it contains olfactory sensory neurons contributing to smelling. With direct access to the central nervous system (CNS) through these neurons, it offers an opportunity to treat neurodegenerative disorders while bypassing the blood-brain barrier (Figure 1.) [16].

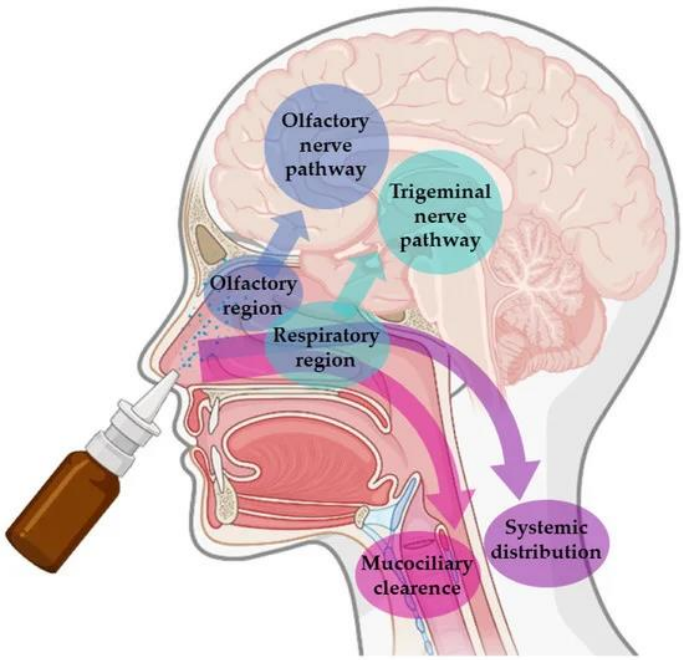

Figure 1. Possible absorption pathways of nasally administered drugs [17]

For a long time, mostly locally acting products have been applied in the nasal cavity to relieve cold and allergy symptoms [18]. In these conditions, the cavernous sinusoids distend with blood causing the swelling of the mucosa resulting in blocked airways. However, the nasal route holds a great potential considering systemic drug delivery. The surface area of the nasal cavity is about 150 cm^2 provided by the cilia and it is highly vascularized in the respiratory region [19]. The drug absorbed into the capillaries through the mucosa, bypasses the first pass hepatic effect and enters the systemic circulation directly. This way, a rapid onset of action is achievable, and the dose of the APIs might be lowered which can moderate the side effects. Furthermore, nasal delivery is a simple, patient-friendly and non-invasive method that enables self-medication and reduces the risk of infections potentially enhancing patient adherence [20].

Although there are several beneficial physiological properties to the nose, drug absorption is multifactorial and can be challenging. One of the major factors is the mucociliary clearance [21]. It is part of the nasal defense system, whose task is to reduce the contact time of the mucosa with bacteria, harmful substances and particles and eliminate them. Accordingly, the respiratory epithelium is covered by an approximately 5 μm thick mucus layer consisting of about 95% water, 2-3% mucin and lipids, electrolytes and proteins in addition, with a pH of 5.5-6.5 [12]. Mucus is negatively charged. This negative charge is primarily due to tpresence of sulphate and carboxyl groups on the mucin molecules, the main gel-forming proteins in mucus. These negatively charged groups are found on the O-linked glycans that extend from the mucin protein backbone [22]. Goblet cells and seromucous glands together are responsible

for the mucus secretion. The ciliated cells propel the mucus towards the nasopharynx thanks to which it is renewed in every 10-20 min [23]. Therefore, the administered drugs have only a limited time to be absorbed. This time can be extended by the application of mucoadhesive, gelling polymers which are able to slow down or hinder the mucociliary clearance to some extent. Moreover, the chosen dosage form can also have an impact on the residence time of the API [24].

The selective permeability of the mucosa is another important factor. The epithelial cells are easily passable for lipophilic molecules by transcellular transport; however, to permeate, they need to be dissolved in the mucus layer that covers the cells. Polar molecules cross the barrier through the paracellular route, and even though they are soluble in the mucus, their absorption can be impaired by their charge and molecular weight, not to mention that they are more prone to the mucociliary clearance [25]. Negatively charged molecules may insufficiently absorb because of the repulsion of the also negatively charged mucosa [26]. Furthermore, the extent of drug absorption is inversely proportional to the molecular weight when it occurs through the tight junctions. Above 300 Da, it may decrease, and APIs greater than 1000 Da exhibit significantly lower permeation rate [27]. Solubilizing and permeation enhancing excipients may provide solutions to the aforementioned problems.

The sensitivity of the mucosa is a non-negligible factor in drug delivery, as well. Irritants increase mucociliary clearance and cause sneezing, which allows these substances to be quickly removed from the nasal cavity [18]. For this reason, it is important to understand the reactions that the API and excipients we intend to deliver may provoke. Acceleration of mucociliary clearance reduces the contact time of the drug with the mucosa thereby hindering its absorption.

The enzymatic activity should also be taken into consideration in some cases. Proteolytic enzymes present in the mucosa cause the degradation, thus inefficient absorption of nasally administered proteins. The application of enzyme inhibitors can improve the bioavailability of these biomacromolecules [28].

Interpersonal variability adds another layer of complexity to nasal drug absorption: structural differences such as the thickness of the epithelium, density of blood vessels, mucus layer characteristics, and expression of metabolic enzymes or efflux transporters result in varying permeability and absorption rates among patients. Furthermore, chronic conditions like rhinitis or nasal polyps can alter mucociliary clearance and enzyme expression, leading to less predictable absorption profiles [29,30]. The variability of nasal mucosa leads to variability in pharmacokinetic profile.

Despite the challenges, the nasal route is a promising alternative route of administration whose limitations can be overcome by choosing the appropriate combination of excipients, dosage form, and formulation techniques.

3.2 Excipients in nasal drug delivery

Excipients can play a major role in outwitting the physiological properties of the nose to induce the desired drug effects. Permeation enhancers are one of the most frequently studied excipient types in intranasal drug delivery. These compounds are used to improve the absorption of the APIs. They either affect the cell membrane permeability by interacting with the tight junctions or increasing the membrane fluidity, or they alter the physicochemical properties of the drugs by solubilizing and/or stabilizing them [31,32]. This group includes – among others – surfactants (e.g. phospholipids, bile salts, fatty acids), cationic polymers (e.g. chitosan, polyethylenamine, cationated gelatins) or cyclodextrins [33,34]. To increase the residence time of the APIs, polymers are another frequently applied excipient group. Typical examples of this group are poloxamers, polyacrylates, hyaluronic acid or cellulose derivatives [10]. Besides, enzyme inhibitors can be important excipients when delivering peptides through the nasal route by decreasing their degradation. For instance, bestatin or puromycin can be used for this purpose [35].

In this section, the excipients applied in this doctoral research work will be introduced.

3.2.1. Cyclodextrins

Cyclodextrins (CDs) are cyclic oligosaccharides built up of D-glucopyranose units. These units link through α-(1-4) glycosidic bonds forming a toroidal shape with a hydrophobic interior and hydrophilic exterior. Their unique structure allows of incorporating hydrophobic compounds into their cavity while keeping their water solubility [36,37]. The so-called parent or native CDs – α-, β- and γ-cyclodextrin (ACD, BCD and GCD) – are composed of six, seven and eight glucopyranose units, respectively. The size of their cavity increases with the amount of linking units resulting in different complexing capabilities. ACD's cavity is suitable for entrapping mostly aliphatic chains, while BCD complexes aromatic rings with high efficiency, many APIs have such aromatic structure causing the popularity of BCD and BCD-derivatives [38]. Parent CDs differ in solubility, the BCD is the least soluble in water due to intramolecular hydrogen bonding. These hydrogen bonds are formed between the C2-OH and C3-OH groups of two neighboring glucopyranose units causing the rigidity of the molecule and reduced capability of forming hydrogen bonds with water molecules [39].

The derivatives of BCD are formed to exploit its advantageous cavity size but increase its water solubility. The hydroxyl groups of the glucopyranose units can be replaced with different substituents, such as hydroxypropyl, sulfobutyl ether or methyl [37]. These groups are randomly bound to the molecule which yields a heterogenous product leading to an amorphous structure in contrast to the native CDs which have crystalline structure. The randomly linked new functional groups also break the amount of intramolecular hydrogen bonds resulting in improved solubility or – depending on the substituent – different toxicity from the parent CDs [3,40].

CDs are widely used in the pharmaceutical industry because of their capability of entrapping hydrophobic molecules in their cavity thereby enhancing their solubility, stability and bioavailability. The growing amount of marketed product which contain CDs shows their significance: they are applied in almost all type of dosage forms including tablets, injections, eye drops, suppository or ointments among others [41]. Furthermore, some of the CDs have been recognized as a potential API. Hydroxypropyl-β-cyclodextrin (HPBCD) is currently being tested in Phase III clinical trial for the treatment of Nieman Pick Type C disease [42], sugammadex is used for the reversal of neuromuscular block under anesthesia and the testing of a dimerized CD on humans for the treatment of atherosclerosis regression has been initiated [43].

As excipients, BCD and its derivatives are the most common types [41]. Often, their role in the formulations is to improve the bioavailability of lipophilic APIs by increasing their solubility [44]. Although, the bioavailability enhancing property of the CDs may also prevail due to their absorption enhancing feature [45]. CDs are considered to increase the permeation rate through different mechanism of actions. On the one hand, they extract cholesterol, phospholipids and other lipophilic components from the cell membrane which are responsible for the rigidity. By that, the membrane fluidity increases which facilitates drug absorption as it reduces the energy barrier for the permeating APIs [46]. On the other hand, they have an impact on tight junctions, but the background of this observation has not been clarified yet [47]. Apart from solubility and permeation enhancing properties of CDs, they may act as dissolution rate enhancers through improving the wettability of powders [48,49]. The above-described positive effects result in an overall higher absorbed quantity of the administered API, i.e. less API is needed for the same efficacy, consequently, the side effects can be reduced.

In nasal dosage forms, CDs can be particularly useful. Because of the previously detailed physiology of the nose, the delivered drugs have only a limited time for absorption, therefore, it is highly important that they dissolve quickly in the mucus and diffuse through the epithelial

layer as fast as possible into the circulation. Although only two nasal products have been marketed that contain CD as an excipient [41,50] (Table 1.), it shows their great potential that several studies have focused on the bioavailability or efficacy enhancement of different APIs by applying CDs recently. For instance, nasal powder formulations of thalidomide – an anti-epistaxis agent – and different BCDs for local action were tested for patients with recurring nose bleeding [51]. In other studies, metoclopramide hydrochloride, midazolam, carfentanil and melatonin were formulated applying different CDs for systemic action induction through the nose [52–55]. For the treatment of neurological disorders, idebenone, tacrine and deferoxamine mesylate were studied in the presence of CDs aiming nose-to-brain delivery [56–58]. These examples highlight CDs as potentially valuable tools for local, systemic and nose-to-brain drug delivery through different mechanisms.

Table 1. Approved nasal products containing CD [41,50]

Product	**Aerodiol® (Eli Lilly, Indianapolis, IN, USA)**	**Baqsimi™ (Servier, Suresnes, France)**
API	17β-estradiol hemihydrate	Glucagon
CD	Randomly methylated BCD	BCD
Other excipients	NaCl, NaOH, HCl, purified water	Dodecylphosphocholine
Dosage form	Nasal spray	Nasal powder
Indication	Hormone replacement therapy	Severe hypoglycemia

3.2.2. Polymers

Polymers are macromolecules consisting of repeating subunits called monomers connected by covalent bonds. They can be classified based on different characteristics, e.g. their origin – natural, semi-synthetic and synthetic; their degradability – biodegradable and non-biodegradable; or chain structure – linear, branched, crosslinked or network [59]. Their utilization in the pharmaceutical field is divers: they are applied as viscosity controlling excipients for suspensions, film coatings for tablets, drug release controllers, mucoadhesive agents or scaffolds for tissue engineering [60]. Their suitability for pharmaceutical purposes is affected by their molecular weight, solubility, swelling behavior, degradation, bioadhesive potential, erosion mechanism and biocompatibility [61].

Water-soluble polymers are particularly popular choice of excipients in dosage forms because of their capability for drug solubilization and stabilization, thus bioavailability enhancement [62]. In nasal formulations, their role in addition is the prolongation of the residence time of the API on the mucosal surface by providing bioadhesion and counteracting the mucociliary clearance [63].

Mucoadhesion has a complex mechanism that is described by several theories, however, none of the theories expresses sufficiently the phenomenon on its own, multiple of them should be interpreted simultaneously for its complete explanation in the case of different dosage forms. These are the electronic, wetting, adsorption, diffusion, dehydration, fracture and mechanical theories [64,65].

- According to the electronic theory, at the interface of the polymer and the tissue, an electrical double layer is formed because of the occurring electron transfer caused by the electronic structure differences between the bioadhesive and the glycoprotein chains of the mucus. In this case, adhesion is due to the attractive interactions developed across the double layer [66].
- The wetting theory analyses the spreading and adhesion capability of liquids and semi-solids over a biological surface measuring the surface and interfacial tension. The adhesive work can be calculated based on these parameters [67].
- The adsorption theory explains mucoadhesion by the formation of secondary interactions – Van der Waals forces, hydrogen bond or hydrophobic interaction – between the polymer and the mucus [68].
- Based on the diffusion theory, adhesion occurs due to the interpenetration of the polymer chains into the mucus. The entanglement of the polymer chains into the mucus creates a semi-permanent adhesion [64].
- According to the dehydration theory, when a dry formulation is brought into contact with the mucus layer, it will absorb water quickly because of the occurring osmotic pressure difference dehydrating the mucus layer. As a result of dehydration, adhesive bond is formed [69].
- The fracture theory assumes that the force needed for the separation of two surfaces is equal to the adhesive strength and that fracture occurs exactly at the contacting surfaces. It is mainly applicable for rigid formulations [70].
- Mechanical theory assumes that the irregular rough or abrasive substrate surface provides mechanical keying [65].

Mucoadhesive polymers can be classified based on the mechanism of binding: there are non-covalent and covalent binding polymers. Non-covalent binding polymers can be anionic, cationic and non-ionic [71].

Anionic polymers are mostly carboxylic acid moieties that can adhere through hydrogen bonding to the mucosal surface. For instance, alginate, carbomer and hyaluronic acid are anionic polymers. Hyaluronic acid has been tested and applied in nasal formulations for several years, in addition to its mucoadhesive feature, its biocompatibility, biodegradability and viscoelasticity contributes to its frequent application in nasal drug delivery systems [72]. Moreover, according to a meta-analysis, it can significantly reduce the symptoms of nasal inflammatory diseases [73]. These data prove that the negatively charged polymers can also be mucoadhesive despite the repulsive forces between mucin and their side chains due to their other moieties than charged functional groups.

The strong adhesion potential of cationic polymers is due to their ionic interaction with the anionic substructures of the mucus gel. Chitosan is a significant member of this group which exhibits not only mucoadhesive property, but also permeation enhancing feature [74,75].

Non-ionic polymers are assumed to present mucoadhesion because of chain interpenetration-entanglement and hydration related swelling beside the H-bond and Van der Waals forces, however, they are described as moderately mucoadhesive compounds. Popular examples of non-ionic polymers are cellulose derivates, poloxamers or polyvinyl alcohol (PVA) [76]. PVA is a synthetic water-soluble polymer that is used as a stabilizer in emulsions and suspensions [77]. It also helps to form spherical morphology for powder particles and can decrease the cohesion between the particles improving powder flow properties [78]. Although PVA exhibits moderate mucoadhesiveness, it can increase the viscosity of the formulation as a result of swelling during its dissolution at the action site [79]. The viscous formulations can have higher residence time on the nasal mucosa.

Beyond the solubilizing and mucoadhesive properties of polymers and their contribution to controlled drug release profiles, their combination with CDs can be particularly advantageous. In the presence of hydrophilic polymers, co-complexes are formed with the CDs and the drug molecule [80]. This way the complexing efficacy and the stability of CD-drug complexes can increase resulting in smaller quantity of CD for the same solubilizing effect [81].

3.3 Nasal dosage forms – powders

Liquid, semi-solid as well as solid nasal dosage forms are available on the market. Nowadays, the most used nasal formulations are liquid – sprays or drops – regardless of the

effect to be induced, because of their quick drug release, ease of use and simple manufacturing [82]. However, their microbiological stability is poor despite the applied preservatives, and they are rapidly forwarded by the mucociliary clearance which reduces drug absorption [83]. Because of that, more frequent dosing might be necessary which affects patient compliance.

Nasal powders, on the contrary, possess low moisture content, due to which there is no risk for hydrolysis and microbial contamination during their storage. Because of this, their production does not require preservatives, which could irritate the mucosa, thus adversely affecting the residence time of the product [84]. They also exhibit prolonged retention in the nasal cavity, and their adhesiveness can be further improved by incorporating bioadhesive polymers [84]. As a result, powders may provide higher local drug concentration and extended time for absorption.

There are several different techniques for the preparation of nasal powders. One part of the methods involves size reduction of greater particles through mechanical stress, e.g. milling or grinding [85]. Although these methods are relatively simple and cost-effective, they may result in a broad particle size distribution unless controlled prudently and there is a risk of metal contamination in the product [86].

Another part of the processes is related to removing the solvent. During lyophilization, the product is cooled below its freezing point and the solvent sublimates under vacuum, then the residual water is removed applying increasing temperature. The resulting powder is stable and dissolves easily in water [87,88]. Furthermore, it is a particularly suitable technique for thermally unstable compounds; however, it is time- and energy-consuming, therefore costly preparation process [89,90].

In contrast to freeze drying, spray drying applies heating to remove the solvent. It provides control over particle size, shape and surface characteristics, which are crucial regarding drug absorption [91]. It is feasible for rapid and scalable production of dry powders from solutions or suspensions. Both mini- and nano spray driers are available for laboratory-scale applications. The liquid feed is transferred into the nozzle by a pump and atomized into fine droplets in the drying chamber. There, they are exposed to heat, and the solvent evaporates forming solid particles. After that, the particles are collected in a cyclone or on an electrostatic collector [92]. Adjusting the process parameters allows us of achieving different particle properties. For instance, a more concentrated liquid feed produces larger, more compact particles. Higher pump rates also result in larger particles because of the formation of larger drops. The atomization parameters such as the nozzle type and the applied pressure influence the size of the formed droplets, thus the particle size: the smaller the droplets are, the smaller the dried particles are,

too [93,94]. Inlet air temperature affects the evaporation rate of the solvent: higher temperature leads to faster drying resulting in wrinkled surface characteristics and porous particles, whereas lower temperature produces smooth-surfaced compact particles [95]. Spray drying often yields amorphous products [96].

Despite the variety of preparation methods for nasal powders, only a limited selection of products is available on the market. Table 2. shows the list of currently accessible formulations. Most of them is for the treatment of local allergic symptoms, only two is intended for systemic action: Onzetra Xsail® and Baqsimi™. Lately, more and more studies have been carried out on nasal powders targeting the systemic circulation. For instance, carvedilol was formulated with chitosan and tested on rabbits with the aim of treating angina pectoris achieving a high absolute bioavailability [97]. Lorazepam, a sedative, was spray-dried with different polymers and administered to rabbits also exhibiting a rapid onset of action in vivo [98]. Another study included 3 different APIs, antipyrine, acyclovir and griseofulvin to compare their nasal absorption from solution, powder and granule form. They emphasized the need for use of excipients that slow down mucociliary clearance in the powder formulations [99]. These findings highlight the growing potential of nasal powders as effective drug delivery systems for systemic effect induction.

Table 2. Marketed nasal powders

Product	API	Dose	Excipient(s)	Device
Atzumi™[100]	Dihydroergotamine mesylate	5.2 mg	Hypromellose, mannitol, microcrystalline cellulose	Single-dose nasal device
Baqsimi™ [101]	Glucagon	3 mg	BCD, dodecylphosphocholine	Single-dose container
Erizas® [6]	Dexamethasone cipecilate	400 μg	Lactose	Capsule-based breath-actuated Multi-dose nasal spray
		200 μg	Lactose	
ONZETRA® Xsail® [102]	Sumatriptan succinate	11 mg/nostril	-	Powder Exhalation Delivery System
Rhinocort® Turbuhaler® [103]	Budesonide	100 μg	-	Multi-dose breath-actuated metering device
Teijin Rhinocort® [103]	Beclomethasone dipropionate	64 μg	HPMC, magnesium stearate, stearic acid	Single dose patient-operated capsule-based device

3.4 Pain management – nasal alternatives

Depending on the intensity and the nature of pain, it is treated with different groups of analgesics.

Mild pain is treated with non-steroidal anti-inflammatory drugs (NSAIDs). NSAIDs act primarily by inhibiting cyclooxygenase (COX) enzymes (COX-1 and COX-2), thereby reducing prostaglandin synthesis [104]. Meloxicam (MX) is a long-acting NSAID of the oxicam class with preferential COX-2 inhibition, offering analgesic and anti-inflammatory effects with reduced gastrointestinal risk compared to non-selective NSAIDs [105]. Its long

half-life (around 20 h) supports once-daily dosing for chronic pain conditions like osteoarthritis [106]. MX is a BCS II class drug, i.e. it has low solubility, high permeability, therefore its bioavailability is limited by its solubility [107]. To improve its aqueous solubility, the salt form of MX, meloxicam potassium (MXP) monohydrate was developed by Egis Ltd. (Budapest, Hungary). It exhibits a higher aqueous solubility (MXP: 13.1 mg/mL in water at 25 °C; MX: 4.4 μg/mL in water at 25 °C) [108]. By using advanced formulation techniques, e.g., spray drying, forming amorphous solid dispersions, incorporating into polymer matrices, its permeability and bioavailability can be further increased [109].

Moderate to severe pain is mostly treated with opioids. Opioid analgesics, such as morphine, fentanyl, and oxycodone act on opioid receptors to inhibit nociceptive transmission and alter pain perception. They are prescribed for postsurgical or cancer pain among others, but their use must be guided by considerations of tolerance, dependence, and respiratory depression risk [110,111].

In addition to the described groups, there are special conditions where other adjuvants are used including local anesthetics, tricyclic antidepressants or triptans. While not primarily developed for analgesia, these agents modulate pain via central sensitization mechanisms and modified neurotransmitter activity [112].

Whether acute or chronic pain, both are predominantly relieved by two routes of administration: per os or intravenously. Oral formulations – as presented earlier – are convenient, self-administered, and suitable for sustained release or chronic pain management. However, they exhibit delayed onset (1-2 hours), variable absorption from GI tract, food effects, and first-pass hepatic metabolism, which reduces bioavailability and increases interpatient variability [113]. Intravenous administration bypasses absorption delays and first-pass metabolism providing rapid and predictable plasma concentrations. It is the preferred solution in emergency, perioperative, or hospital settings but it requires trained personnel, sterile equipment, and venous access [114]. The nasal delivery of analgesics offers a non-invasive, self-administered solution to the above-mentioned limitations because the nasally delivered APIs exert their effect with a short onset, they bypass the first-pass hepatic metabolism improving bioavailability. The nasal products are ideal when patients cannot swallow or need analgesia in settings where intravenous access is impractical [115].

There are several painkiller nasal products available on the market (Table 3.) but only one contains an NSAID (ketorolac tromethamine containing spray) so far and only a few of the presented products are powder formulations. This emphasizes the importance of collecting novel results on such formulations containing NSAIDs.

Table 3. Marketed nasal analgesic products [100,116–122]

API	Marketed product names	Dosage form	Dose per administration
Ketorolac tromethamine	SPRIX®	Nasal spray, solution	15.75 mg per metered spray (100 µL) per nostril (total 31.5 mg)
Fentanyl citrate	Lazanda®, PecFent®, Instanyl®	Nasal spray, solution	50-400 µg per metered spray depending on product and titration
Butorphanol tartrate	Stadol NS®	Nasal spray, solution	1 mg per metered spray
Sumatriptan	Imitrex®, Tosymra®, Onzetra Xsail®	Nasal spray, solution or nasal powder	5–20 mg for the nasal sprays (Imitrex and Tosymra), 11 mg per capsule (Onzetra; both nostrils = 22 mg)
Zolmitriptan	Zomig® Nasal Spray	Nasal spray, solution	2.5 mg or 5 mg per metered spray
Dihydroergotamine mesylate	Atzumi™ Migranal®, Trudhesa®	Nasal powder or nasal spray, solution	0.5-1.45 mg depending on product and titration
Zavegepant	Zavzpret®	Nasal spray, solution	10 mg per metered spray

4. MATERIALS AND METHODS

4.1. Materials

4.1.1. Active pharmaceutical ingredient (API)

Meloxicam potassium (MXP) monohydrate (Figure 2.) was used as the API in this work and was obtained from Egis Ltd. (Budapest, Hungary). It is the potassium salt of meloxicam, which was patented by Egis Ltd. To the best of our knowledge, it has not been incorporated in any marketed product yet.

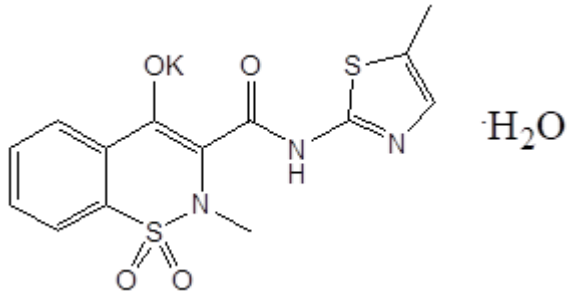

Figure 2. Chemical structure of MXP monohydrate

4.1.2. Excipients

4 different CDs, namely β-cyclodextrin (BCD), (2-hydroxy)-propyl-β-cyclodextrin (HPBCD), sulfobutylated-beta-cyclodextrin sodium salt (SBECD, DS~6) and (2-hydroxy-3-N,N,N-trimethylamino)propyl-beta-cyclodextrin chloride (QABCD, DS~2.7) were all obtained from CycloLab Ltd. (Budapest, Hungary). Sodium hyaluronate (HA) was from Contipro Biotech (Dolní Dobrouč, Czech Republic) and (polyvinyl)alcohol (PVA) was from Sigma Aldrich (Sigma Aldrich Co. LLC, St. Louis, MO, USA). The formula and role in drug delivery of the applied excipients are presented in Table 4.

Table 4. The applied excipients, their formula and their function in drug administration

Excipient	Simplified chemical structure	Function in drug administration
BCD	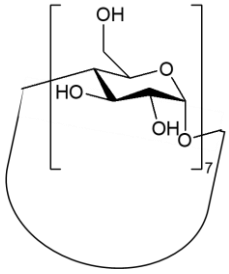	Solubility and permeation enhancer [123,124]
HPBCD	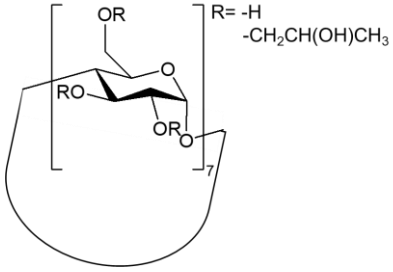	Solubility and permeation enhancer [125,126]
SBECD	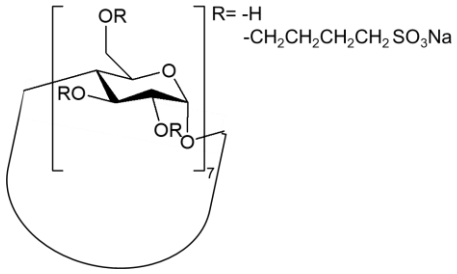	Solubility and permeation enhancer [123,124]
QABCD	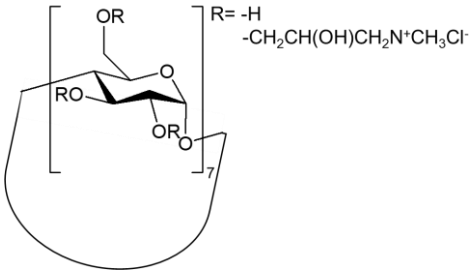	Solubility and permeation enhancer [127,128]
HA	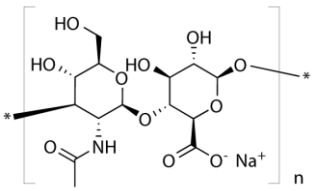	Mucoadhesive agent [129]
PVA	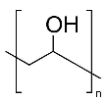	Stabilizer in emulsions and suspensions, mucoadhesive agent [77,130]

4.2. Methods

4.2.1. Preparation method of the spray-dried (SD) samples

BÜCHI Nano Spray Drier B-90 HP (BÜCHI Labortechnik AG, Flawil, Switzerland) (Figure 3.) was used for the preparation of the samples. The feeding solutions for the polymer-free formulations consisted of 1:1 molar ratio of MXP and CD (BCD/HPBCD/SBECD/QABCD) dissolved in distilled water. For the polymer-containing formulations, the solutions additionally included 1 mg/mL PVA or 0.5 mg/mL HA. The following parameters were applied for the spray drying: inlet air temperature: 80 °C, compressed air flow: 130 $L \cdot h^{-1}$, pump rate: 20%, aspirator capacity: 100%.

Physical mixtures (PMs) were prepared as reference samples, maintaining the same ratios as those in the spray-dried solutions. The components were blended using a Turbula mixer (Turbula WAB, Systems Schatz, Muttenz, Switzerland) at 50 rpm for 10 minutes.

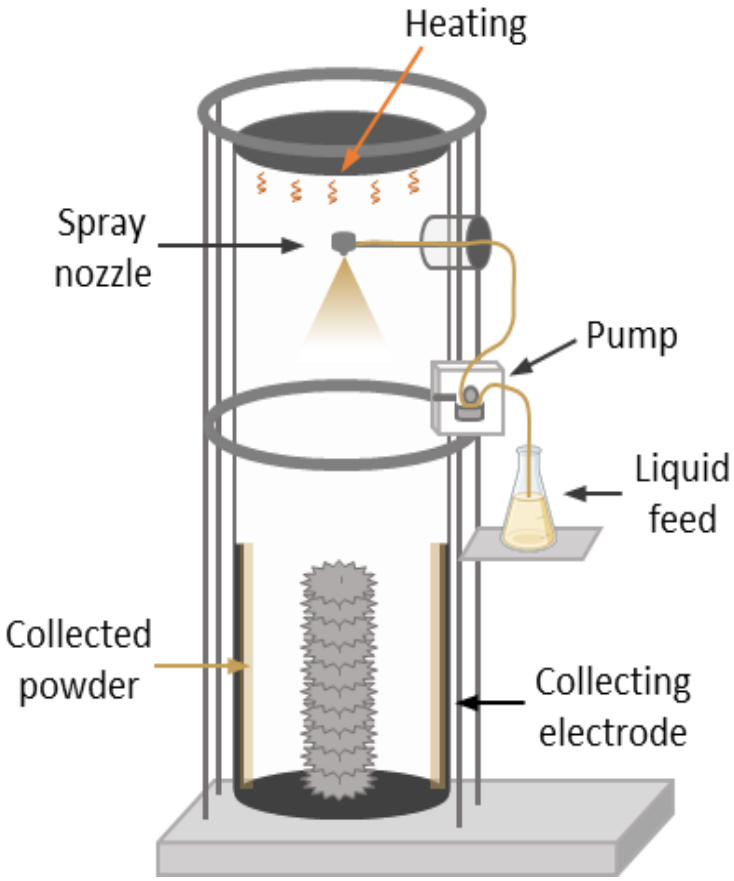

Figure 3. Schematic diagram of the nano spray dryer

4.2.2. Physico-chemical characterization

4.2.2.1. Laser diffraction

The particle size distribution of the spray-dried products was characterized using a Malvern laser diffractometer (Malvern Mastersizer Scirocco 2000; Malvern Instruments Ltd., Worcestershire, UK). Air was used as the dispersion medium during the dry analysis and its pressure was set to 2 bar. Approximately 1 g of each sample was tested, and all samples were measured in triplicate. The particle size was characterized by the D(0.5) value, indicating the diameters below which 50% of the particles by volume are found.

4.2.2.2. Scanning electron microscopy (SEM)

SEM analysis (Hitachi S4700, Hitachi Scientific Ltd., Tokyo, Japan) was conducted to examine the surface characteristics, shape, and size of the prepared particles. The powders were coated with gold-palladium by a sputter coater and analyzed at 10 kV and 10 μA under an argon atmosphere.

4.2.2.3. X-ray powder diffractometry (XRPD)

X-ray diffractograms of the PMs and spray-dried samples were recorded using a BRUKER D8 Advance diffractometer (Bruker AXS GmbH, Karlsruhe, Germany) with Cu K_α radiation (λ = 1.5406 Å), operating at a tube voltage of 40 kV and a tube current of 40 mA. Data were collected over an angular range of 3–40° 2θ, with a step time of 0.1 seconds and a step size of 0.007°. Signal detection was performed with a VÅNTEC-1 detector. The manipulations, including Kα2 stripping, background removal, and smoothing, were conducted using DIFRAC.EVA software.

4.2.2.4. Differential Scanning Calorimetry (DSC)

The thermal behavior of the samples was analysed using a Mettler Toledo DSC 821^e differential scanning calorimeter (Mettler Inc., Schwerzenbach, Switzerland). Samples weighing 2–5 mg were placed in perforated aluminum pans and heated from 25 to 300 °C at a rate of 10 °C·min^{-1} under a constant argon flow of 150 mL·min^{-1}. The recorded DSC curves were analysed using the STAR^e thermal analysis software (Mettler Toledo; Mettler Inc., Schwerzenbach, Switzerland).

4.2.2.5. Fourier transform infrared spectroscopy (FT-IR)

FT-IR measurements were used to detect the interactions between MXP and the excipients. Individual compounds and spray-dried products were measured and compared. The spectra were recorded with an AVATAR330 spectrometer (Thermo Nicolet, Unicam Hungary Ltd., Budapest, Hungary), the interval was in the range of 400–4000 cm^{-1}, at an optical resolution of 2 cm^{-1}. Pastilles prepared from the samples with 0.15 g KBr were investigated. SpectraGryph optical spectroscopy software was used to evaluate and present the detected spectra.

4.2.3. In vitro measurements

4.2.3.1. Texture analyser

The adhesive properties of the formulations were investigated with a TA-XT Plus Texture Analyser (Metron Ltd., Budapest) (Figure 4.) instrument utilizing a cylinder probe with a 1 cm diameter and a 5 kg load cell. Before the measurement, 95±5 mg of the samples was compressed into pastilles with a Specac hydraulic press (Specac Inc., Orpington, UK) applying a pressing force of 10 kN for 10 seconds with a pressing diameter of 13 mm. The pastilles were attached to the cylinder probe and brought into contact with the artificial mucosa layer for 3 minutes at a preload of 2500 mN. After that, the cylinder probe was raised to detach the sample from the filter paper at a speed of 2.5 $mm \cdot min^{-1}$, while a force-distance curve was recorded determining the maximum detachment force and work of adhesion. The latter was calculated as the area under the "force vs. distance" curve. For the artificial mucosa, a filter paper was wetted with 40 µl of an 8% w/w mucin dispersion prepared with simulated nasal electrolyte solution (SNES). Control measurements were performed using SNES-wetted filter papers to observe the behavior of the powders without mucin. For statistical analysis, one-way ANOVA with Tukey's multiple comparison test was applied using Minitab statistical software. A level of $p \leq 0.05$ was considered as significant.

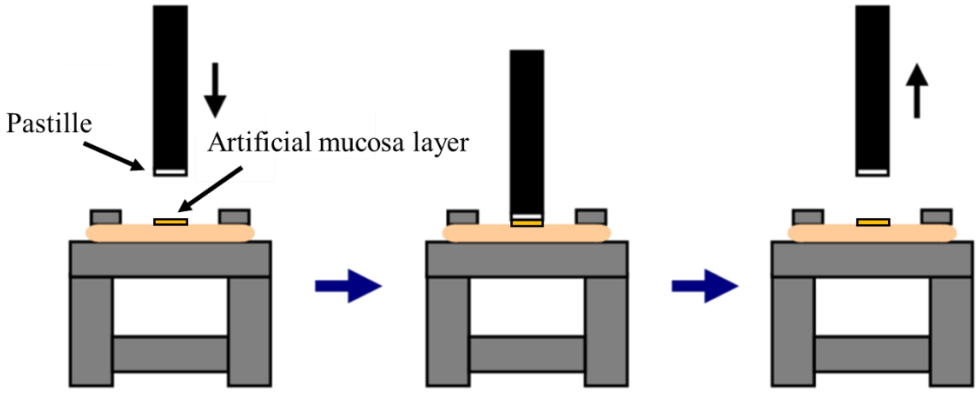

Figure 4. Setup of the adhesion measurements [131]

4.2.3.2. Drug release study modelling nasal conditions

The drug release from the samples was monitored in-line over a period of 5 minutes at a wavelength of 364 nm by adding powders containing 0.75 mg of the API into 50 mL of SNES. The system was maintained at 32 ± 0.5 °C with a constant stirring of 100 rpm. The results were quantified using an AvaLight DH-S-BAL spectrophotometer (Avantes, Apeldoorn, Netherlands) connected to an AvaSpec-2048L transmission immersion probe (Avantes) via an optical fiber.

4.2.3.3. Permeation study through an artificial membrane

A modified horizontal diffusion cell was used to test the *in vitro* diffusion of MXP under nasal conditions and to identify promising formulations for further stability and cell line investigations. The device consisted of two chambers – one for the donor phase and one for the acceptor phase – separated by an artificial membrane. The donor phase contained 9 mL of SNES, representing the nasal fluid, while the acceptor phase contained 9 mL of phosphate buffer solution (pH 7.4) to simulate blood pH (Figure 5.) Both phases were maintained at 32 °C (Thermo Haake C10-P5, Sigma Aldrich Co.) and stirred at 300 rpm using a magnetic stirrer to simulate the airflow and the cilia. To simulate the lipophilic mucosa, a Whatman™ regenerated cellulose membrane filter with 0.45 μm pores was soaked in isopropyl myristate for 30 minutes before the test. Samples containing 7.5 mg of MXP were added to the donor phase at the beginning of the study. Aliquots were collected at predetermined intervals from the acceptor phase and the cumulative amount of permeated MXP was quantified. For statistical analysis, one-way ANOVA with Fisher's multiple comparison test was applied using Minitab statistical software. A level of $p \leq 0.05$ was considered as significant.

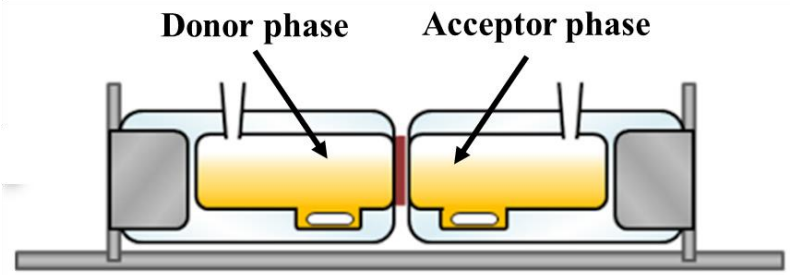

Figure 5. Modified horizontal diffusion cell

4.2.4. Accelerated stability test of the selected samples

The stability of the selected formulations was studied under the accelerated stability test conditions according to the ICH Q1A (R2) guideline. The powders were filled into hydroxypropyl-methyl cellulose (HPMC) capsules and placed into a Binder KBF 240 (Binder GmbH Tuttlingen, Germany) constant-climate chamber without secondary packaging maintaining 40 ± 2 °C and 75 ± 5% RH. The formulations were re-examined after 1 month in terms of morphology, crystallinity and drug content. The results of the stability test contributed to the selection among the formulations for further cell culture measurements.

4.2.5. Cell-based measurements

4.2.5.1. Cytotoxicity of the formulations on RPMI 2650 cells

To evaluate the viability of RPMI 2650 cells, the CellTiter 96® AQueous Non-Radioactive Cell Proliferation Assay (Promega GmbH, Mannheim, Germany) was employed. Cells were cultured and seeded into 96-well plates at a density of 5×10^4 cells per well and maintained until confluence. Test samples - including raw MXP, BCD, SBECD, QABCD alone and BCD-MXP-PVA-SD, SBECD-MXP-PVA-SD, QABCD-MXP-PVA-SD formulations - were added at various concentrations: the CDs in 5, 2.5 and 1 mM concentration, raw MXP in 125, 95, 65, and 25 µg/mL, and the formulations in 125, 95 and 65 µg/mL MXP concentration. The cells were incubated with the solutions for 1 hour at 37 °C. After treatment, the cells were washed with Hank's Balanced Salt Solution and incubated with the MTS reagent for 2 hours at 37 °C. Absorbance was measured at 491 nm using a UV/VIS microplate reader.

For assessment of membrane integrity, lactate dehydrogenase (LDH) release was quantified using the CytoTox-ONE™ Homogeneous Membrane Integrity Assay (Promega GmbH, Mannheim, Germany). Fluorescence was recorded at an excitation wavelength of 560 nm (emission wavelength: 590 nm) using a plate reader. Untreated cells served as negative controls, and lysed cells served as positive controls. Background was subtracted from all measured values

to ensure accuracy. For statistical analysis, one-way ANOVA with Dunnett's test was applied using Minitab statistical software. A level of $p \leq 0.05$ was considered as significant.

4.2.5.2. Drug permeation through nasal RPMI 2650 cell model

The diffusion of MXP from the selected PVA-containing formulations was studied on an RPMI 2650 epithelial cell model cultured under air-liquid interface (ALI). For the model, RPMI 2650 cells at a density of 50,000 cells per 0.33 cm² were seeded onto Transwell™ filter inserts (3 µm pore size, polycarbonate). The cells were cultured in a liquid-covered state for 8 days with refreshing the medium (MEM supplemented with 10% FBS, 1% Penstrep, and 1% non-essential amino acids) every 2–3 days. After 8 days, the inserts were raised to an ALI and cultured for an additional 2-3 weeks to ensure full differentiation of the cells.

The setup of the diffusion test is presented in Figure 6. For the test, BCD-MXP-PVA-SD, SBECD-MXP-PVA-SD and QABCD-MXP-PVA-SD samples were dissolved in phosphate buffer (PBS, pH 7.4) to reach a non-toxic MXP concentration. The same concentration of raw MXP in PBS (pH 7.4) was applied as a control. 600 µL of PBS (pH 7.4) was added to the basolateral compartment, and to start the permeation studies, 100 µL of the sample solutions was added to the apical side of the Transwell™ insert. Samples were taken from the basolateral side at specific time points (5, 10, 15, 30, 45, and 60 minutes) to measure the permeation of MXP across the epithelial layer. The solutions from the apical side were also collected to assess the decrease in API content after 60 minutes. The HPLC method described in section 4.2.6. was used for the determination of MXP-content. For statistical analysis, one-way ANOVA with Fisher's multiple comparison test was applied using Minitab statistical software. A level of $p \leq 0.05$ was considered as significant

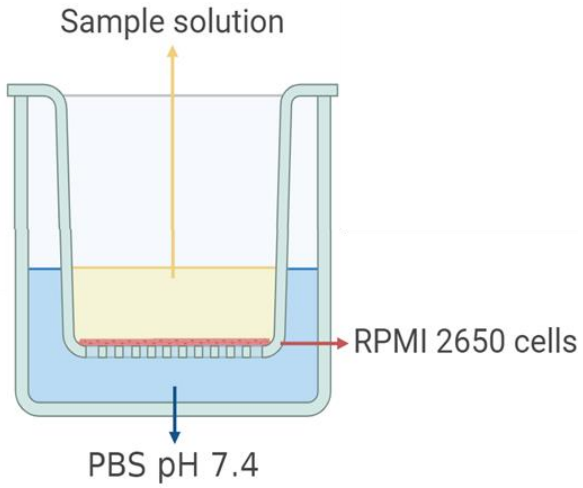

Figure 6. Setup of the permeation study applying RPMI 2650 cells

4.2.6. MXP-content determination by high performance liquid chromatography (HPLC)

An Agilent 1260 HPLC system (Agilent Technologies, San Diego, United States) was used to quantify the MXP amount in the samples. The mobile phase consisted of PBS (pH=2.8) and methanol in a ratio of 42:58 (% v/v). A Kinetex® EVO 5 µm C18 100 Å column (150 x 4.6 mm, Phenomenex, Torrance, CA, USA) was used for the separation. The injection volume for the samples was 10 µL and the separation was performed with an isocratic method, with the flow rate of 1 $mL \cdot min^{-1}$ for 6 minutes at 30 °C. MXP was quantified at 364 nm using a diode array detector. Data were evaluated with ChemStation B.04.03. software (Agilent Technologies, Santa Clara, CA, USA).

5. RESULTS AND DISCUSSION

5.1. Physico-chemical characterization of the prepared samples

5.1.1. Particle size and morphology of the spray-dried samples

Laser scattering was applied for the determination of the particle size. The average particle size was between 1.89 and 3.05 μm (Table 5.). Although particles larger than 10 μm are retained most effectively in the nasal cavity when using nasal powders, the nasal physiological function is to filter out particles as small as 0.5 μm and prevent them to get to the lungs [132]. In addition, the type of delivery device significantly influences powder deposition patterns [133]. Bi-directional devices offer promising opportunities to target smaller particles to the nasal cavity while minimizing lung deposition.

Table 5. D(0.5) values of the samples

Sample	D(0.5) (μm)
BCD-MXP-SD	1.89 ± 0.09
BCD-MXP-PVA-SD	1.97 ± 0.06
HPBCD-MXP-SD	2.72±0.09
HPBCD-MXP-PVA-SD	2.58±0.21
HPBCD-MXP-HA-SD	3.05±0.15
SBECD-MXP-SD	2.21 ± 0.06
SBECD-MXP-PVA-SD	2.14 ± 0.03
QABCD-MXP-SD	2.10 ± 0.03
QABCD-MXP-PVA-SD	1.89 ± 0.06

Based on the SEM analysis, the spray-dried particles consistently demonstrated a uniform, spherical shape and smooth surface characteristics, some submicron-sized particles were also noticeable on them, the images are presented in Figure 7. Such spherical morphology is achieved during spray drying when the rate of the drying process is moderate. In contrast, rapid solvent evaporation – particularly in the presence of polymers – results in more collapsed, shrinked surface characteristics. The Peclet number, which characterizes the rate of the solvent evaporation, correlates to the drying rate: higher Peclet number indicates quicker drying often

resulting in hollow surface characteristics [134,135]. Our spray drying conditions resulted in lower Peclet number forming smooth surfaced particles.

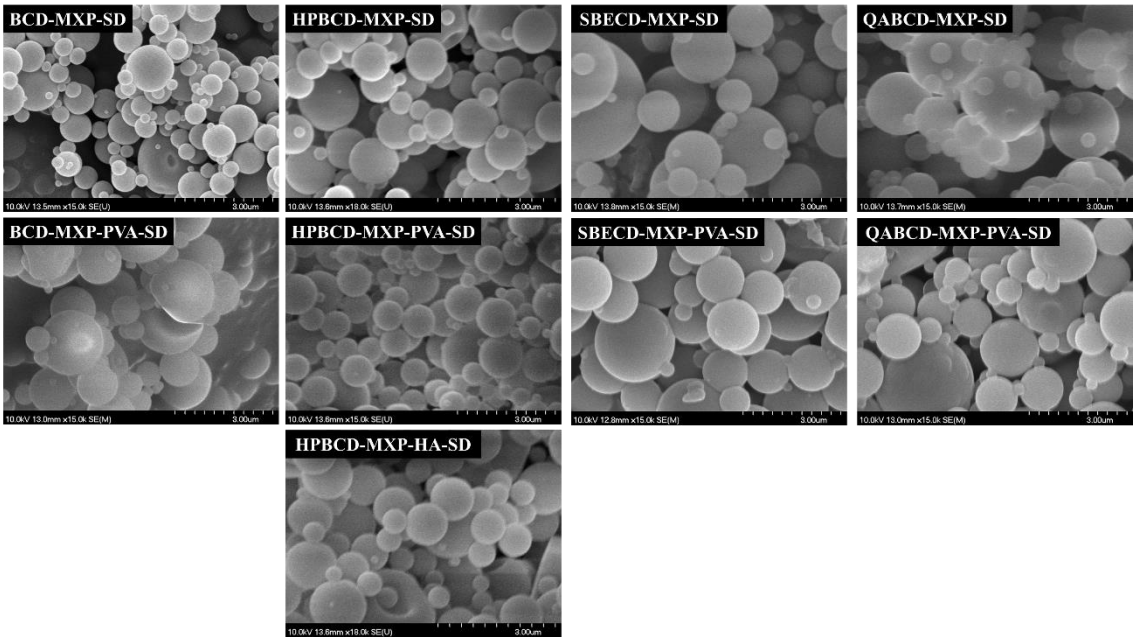

Figure 7. SEM images of the spray-dried samples

5.1.2. Crystallinity of the samples

The crystallinity of the spray-dried samples and PMs was examined by XRPD, the diffractograms are presented in Figure 8. In all PMs, the peaks of the initially crystalline MXP were detected at 2θ of 6.1, 15.5 and 24.6° [109]. The characteristic peaks of BCD appeared at 4.5, 9.0, 10.7 and 12.5° [136], indicating its initially crystalline structure also, which is common for the "parent cyclodextrins". Considering the substituted CDs and the polymers, their diffraction pattern could not be detected suggesting their amorphous state.

In the spray-dried samples, all the previously observed peak disappeared referring to the complete amorphization of every originally crystalline material. This probably occurred due to the preparation process: spray drying often results in the amorphization of the products due to the lack of time for the formation of crystal lattice because of the quick drying process. Our formulations can be considered solid dispersions regardless of whether complex formation had occurred. Solid dispersions usually exhibit improved dissolution [137], which – in our case – would be a desirable outcome of the preparation process, given that most of the nasally applied formulations are removed quickly from the nasal cavity because of the mucociliary clearance. However, the amorphous state may raise concern about the physical stability of the products, which needs to be monitored [138].

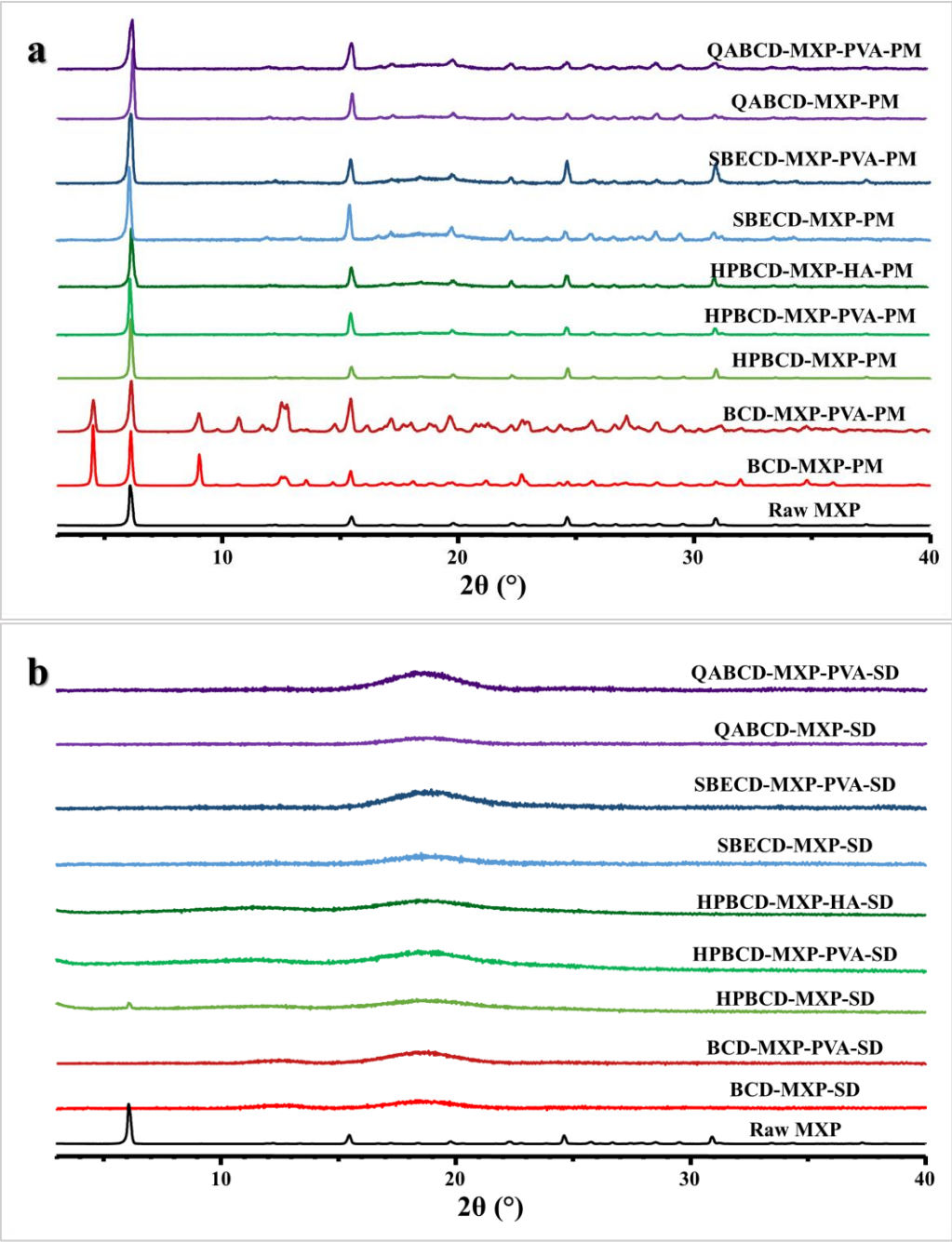

Figure 8. Diffractograms of (**a**) the PMs and (**b**) the spray-dried samples

5.1.3. Thermal behavior of the samples

DSC was used to investigate the thermal behavior of both the spray-dried samples and the PMs, Figure 9. presents the thermograms. In the PMs, the presence of sharp endothermic peaks around 160-170 °C, corresponding to the melting point of MXP, confirmed its crystalline nature. Additionally, an exothermic peak above 245 °C was observed attributed to the decomposition of the drug [139]. The broad endothermic bands between 40 and 150 °C referred to the dehydration of the CDs [140]. Besides, no thermal event was observed in the examined

temperature range except for SBECD. SBECD presented an endothermic peak at 274 °C followed by an exothermic peak at 280 °C, both attributed to its decomposition [141].

In contrast to the PMs, the melting peak of MXP disappeared from the thermograms of the spray-dried samples and the peak of its decomposition also shifted, broadened and diminished indicating the amorphization of MXP in the formulations. The results of the DSC corresponded to that of the XRPD.

The preparation procedure resulted in amorphization of the initially crystalline materials leading to solid dispersions. Due to the lack of crystal lattice, a potential dissolution rate enhancement of the API is expected because no energy is required to break the structure during dissolution anymore [96].

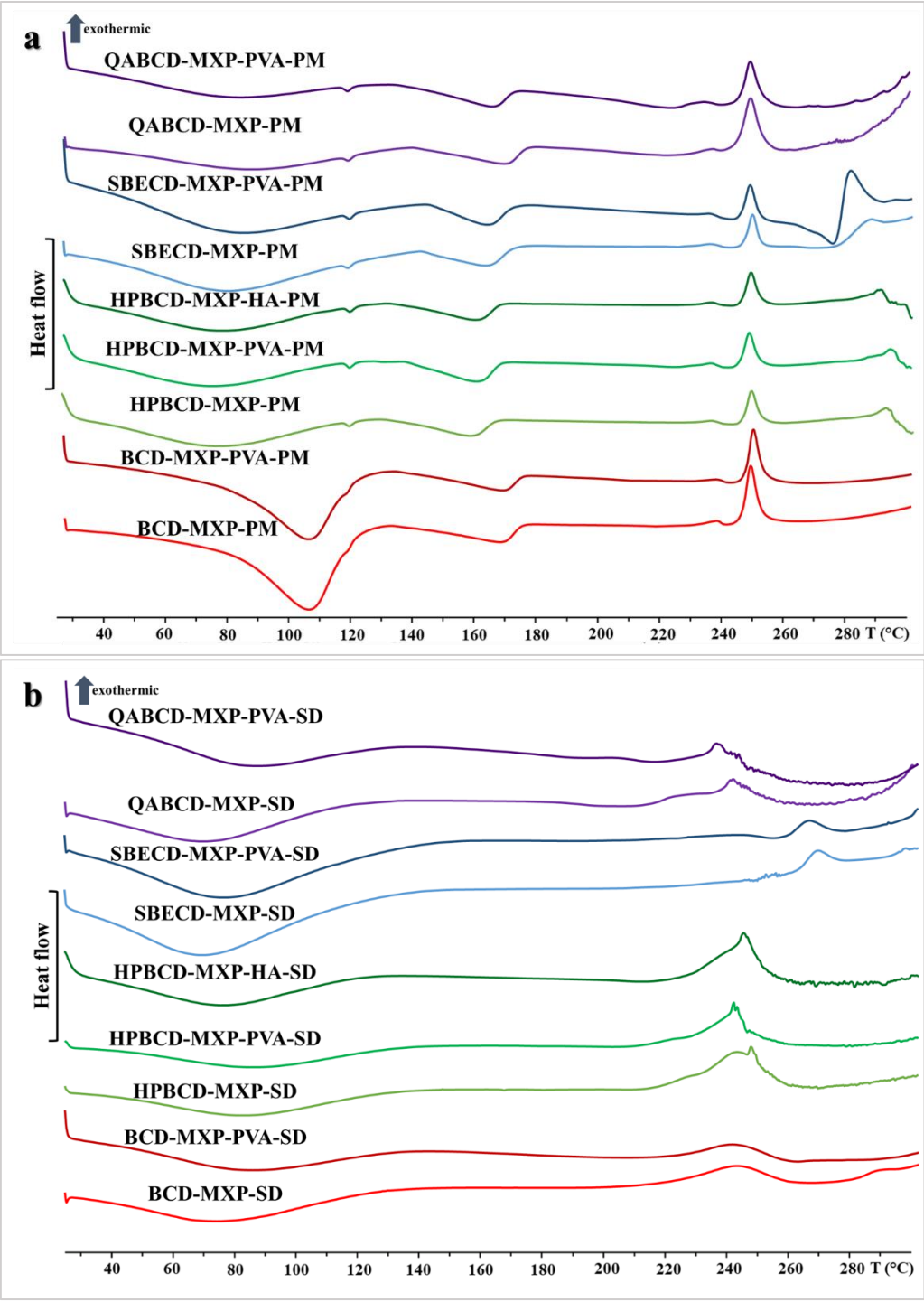

Figure 9. Thermograms of (**a**) the PMs and (**b**) the spray-dried samples

5.1.4. Secondary interactions in the formulations

FT-IR measurement was implemented to study the possibly formed secondary interactions between the excipients and the drug. The individual compounds were compared to the prepared spray-dried samples, the spectra are presented in Figure 10.

MXP exhibited the typical peak of C=O from the amide bond at 1618 cm^{-1} [142]. In the spectra of the CDs, the peak assigned to the O–H stretching was observed in the 3790–3000 cm^{-1} wavenumber range and the peak of O–H bending appeared at 1640 cm^{-1}, 1653 cm^{-1}, 1647 cm^{-1} and 1598 cm^{-1} for BCD, HPBCD, SBECD and QABCD, respectively [143–145].

In the spray-dried formulations, the main event that could be observed was the appearance of a merged, shifted sharp peak in the 1650–1550 cm^{-1} wavenumber range. All BCD- and HPBCD-containing formulations exhibited it at 1616 cm^{-1} and the SBECD-containing formulations at 1623 cm^{-1}. This indicates the potential engagement of the API and the excipients in hydrogen bonding. The shifting occurred regardless of the presence of PVA and HA, their effect might have been shaded because of the low polymer-content of the samples.

Comparing the corresponding individual compounds to the spray-dried QABCD-containing formulations, no change was observed in the spectra indicating the absence of secondary interactions; however, this measurement method is not able to detect the possibly formed electrostatic interaction between MXP and QABCD in the formulation.

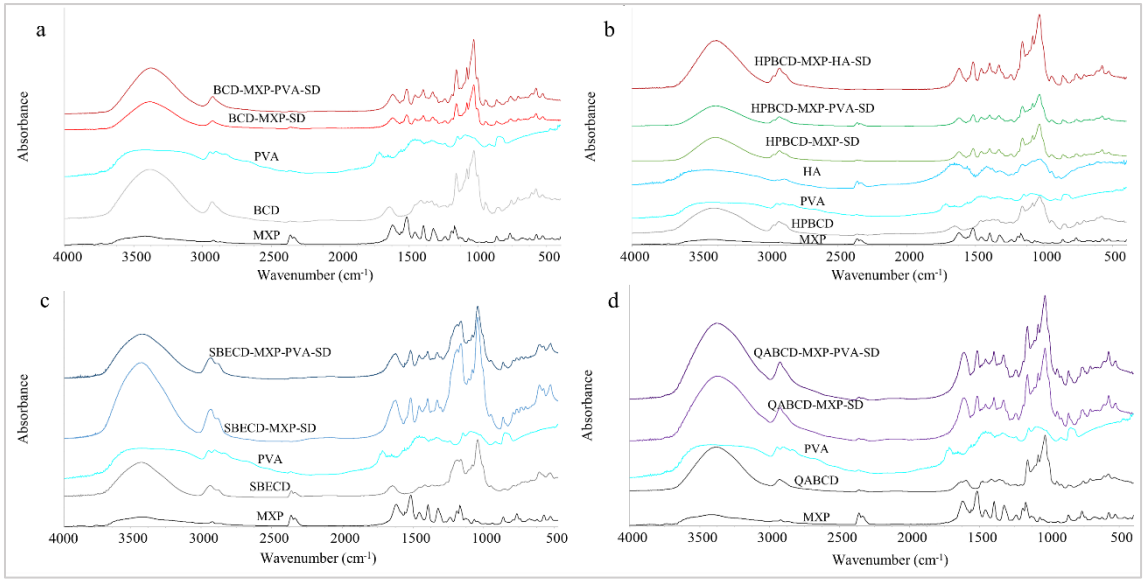

Figure 10. FT-IR spectra of the individual compounds and (**a**) BCD-related samples, (**b**) HPBCD-related samples, (**c**) SBECD-related samples and (**d**) QABCD-related samples

5.2 *In vitro* measurements

5.2.1. In vitro mucoadhesion test

A texture analyser was applied to mimic and test the adhesion of the powders to the nasal mucosal surface. Conclusions were made based on the recorded maximum detachment force and work of adhesion values, which are presented in Figure 11.

Considering maximum detachment force, significantly higher values were detected for each type of sample when contacting mucin compared to SNES. Furthermore, in the presence of mucin, every CD-based sample was significantly different from raw MXP except for BCD-MXP-SD. The polymer content did not affect the peak force, neither PVA nor HA showed a significant effect. Maximum detachment force demonstrates the maximum force required to separate two surfaces and it is associated with the strength of secondary interactions formed between the mucus and the applied materials [146]. Thus, the presence of the CDs was necessary for the formation of these interactions except for BCD, while the same could not be determined with certainty for the polymers.

As for the work of adhesion, in most of the cases no significant difference was found between the mucin and SNES contacting samples, so general conclusions could not be established. However, the measured values were similarly high to a mucoadhesive cysteine-chitosan conjugate prepared and examined for nasal application by Kiss et al [147]. Work of adhesion is considered to reflect both the physical interpenetration and entanglement of the polymer chains and mucin along with the strength of secondary interactions [146]. In our case, the reason of the detected high work of adhesion values was probably the water uptake of the samples. Presumably, after the wetting and swelling of the powders, the liquid was absorbed quickly through the capillaries of the pastilles when contacting the filter papers. This process likely resulted in the dehydration of the artificial mucosal surface thereby creating a strong physical adhesion irrespective of mucin's presence. Our observation suggests that the samples may initially display significant adhesive strength to the nasal mucosa prior to their dissolution.

In summary, the presence of the CDs – except for BCD – was essential for establishing secondary interactions with mucin, moreover, the powders may exhibit a strong adhesion upon initial contact with the mucosa. While this measurement did not confirm the advantageous role of the polymers, their inclusion in nasal formulations could provide enhanced viscosity at their application site potentially decelerating the mucociliary clearance.

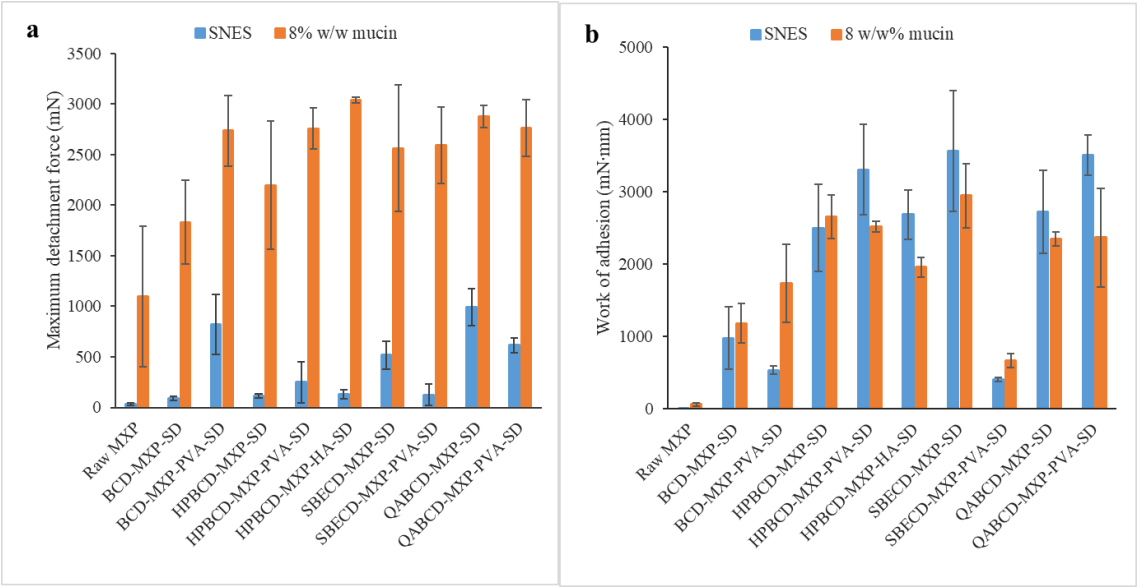

Figure 11. (**a**) Maximum detachment force and (**b**) work of adhesion values

5.2.2 In vitro dissolution of MXP from the samples

The MXP dissolution from the samples was monitored *in-line* applying nasal conditions, the results are presented in Figure 12. Raw MXP, used as a reference, dissolved significantly slower than any other formulation, only 46% of it was detected in the solution after 5 min. In contrast, all spray-dried formulations achieved nearly complete dissolution within the first minute. The applied polymers did not have a noticeable impact on the dissolution rate.

The experienced rapid API dissolution can be attributed to multiple contributing factors, including particle size reduction, amorphization of MXP in the products and the presence of highly water-soluble CDs, which could improve the wettability of the formulations [148]. Since drug absorption through the nasal mucosa requires the API to be dissolved in the mucus [13], faster dissolution may lead to enhanced bioavailability because of the higher concentration gradient.

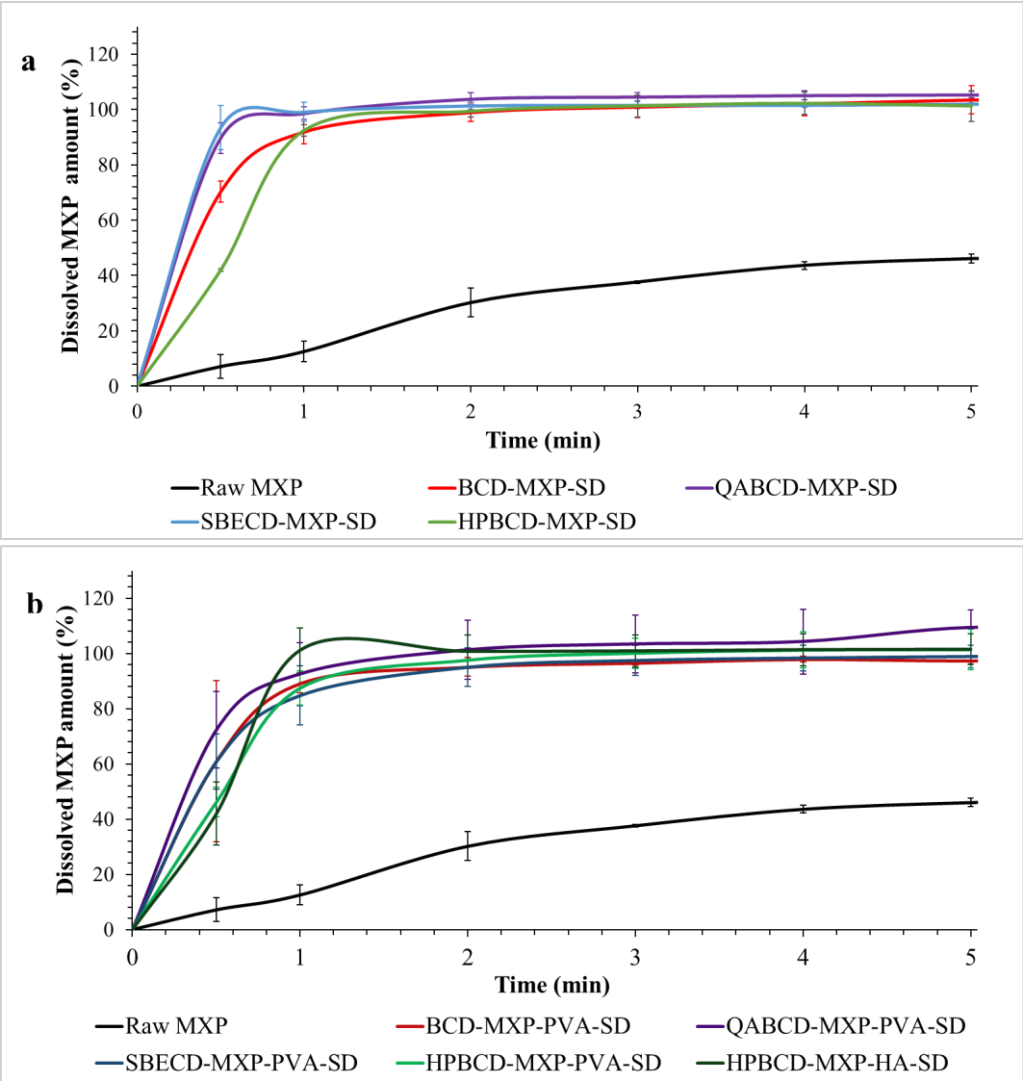

Figure 12. *In vitro* MXP release from the (**a**) polymer-free and (**b**) polymer-containing formulations

5.2.3 In vitro permeation studies applying an artificial mucosa

A horizontal diffusion model with an artificial mucosa was applied to test the *in vitro* diffusion of the samples, Figure 13. presents the results. Raw MXP was selected as a reference compound, from which 54.6 $\mu g \cdot cm^{-2}$ diffused to the acceptor phase within the 1-hour period. Among the polymer-free samples, the highest extent of drug permeation was observed from the cationic QABCD-based formulation, with a significantly greater amount – 208 $\mu g \cdot cm^{-2}$ – compared to raw MXP and the other three formulations. Notably, BCD-MXP-SD, HPBCD-MXP-SD and SBECD-MXP-SD showed similar drug diffusion values, 96.4, 91.9 and 85.3 $\mu g \cdot cm^{-2}$, respectively, without statistically significant differences from raw MXP.

Considering the polymer containing samples, HA-content seemed to be favorable in the HPBCD-based sample, it exhibited a significantly higher permeation rate compared to raw MXP and the polymer-free samples, but significantly lower than the PVA-containing samples. In the presence of PVA, all CD-based formulations demonstrated markedly enhanced permeation rates. QABCD-MXP-PVA-SD exhibited an outstanding diffusion rate of 316.3 $\mu g \cdot cm^{-2}$. The BCD, HPBCD- and SBECD-based PVA-containing formulations also showed high permeation values, 215.3, 194.2 and 205.3 $\mu g \cdot cm^{-2}$, respectively, which were nearly equivalent to the PVA-free QABCD-MXP-SD formulation. These findings highlight the influence of both the cyclodextrin's type and the presence of PVA on API permeation.

QABCD significantly enhanced MXP permeation relative to BCD, HPBCD and SBECD. We hypothesize that electrostatic interactions contributed to the improved permeation: upon dissolution, MXP dissociates into potassium ions and anionic meloxicam, which can interact favorably with the cationic moieties of QABCD. This interaction likely plays a key role in the observed increase in diffusion.

Overall, PVA consistently exhibited beneficial effect on the permeated drug quantity under simulated nasal conditions, it outperformed HA. The dissolution rate did not appear to be the rate-limiting step in diffusion, as all formulations released the drug rapidly. It should be noted, however, that the current diffusion model only permits evaluation of passive diffusion across the artificial membrane, which does not mimic intercellular interactions.

For further experiments, the PVA-containing samples were selected to gain more insight into their stability and the potential permeation-enhancing properties of the CDs on a nasal cell line.

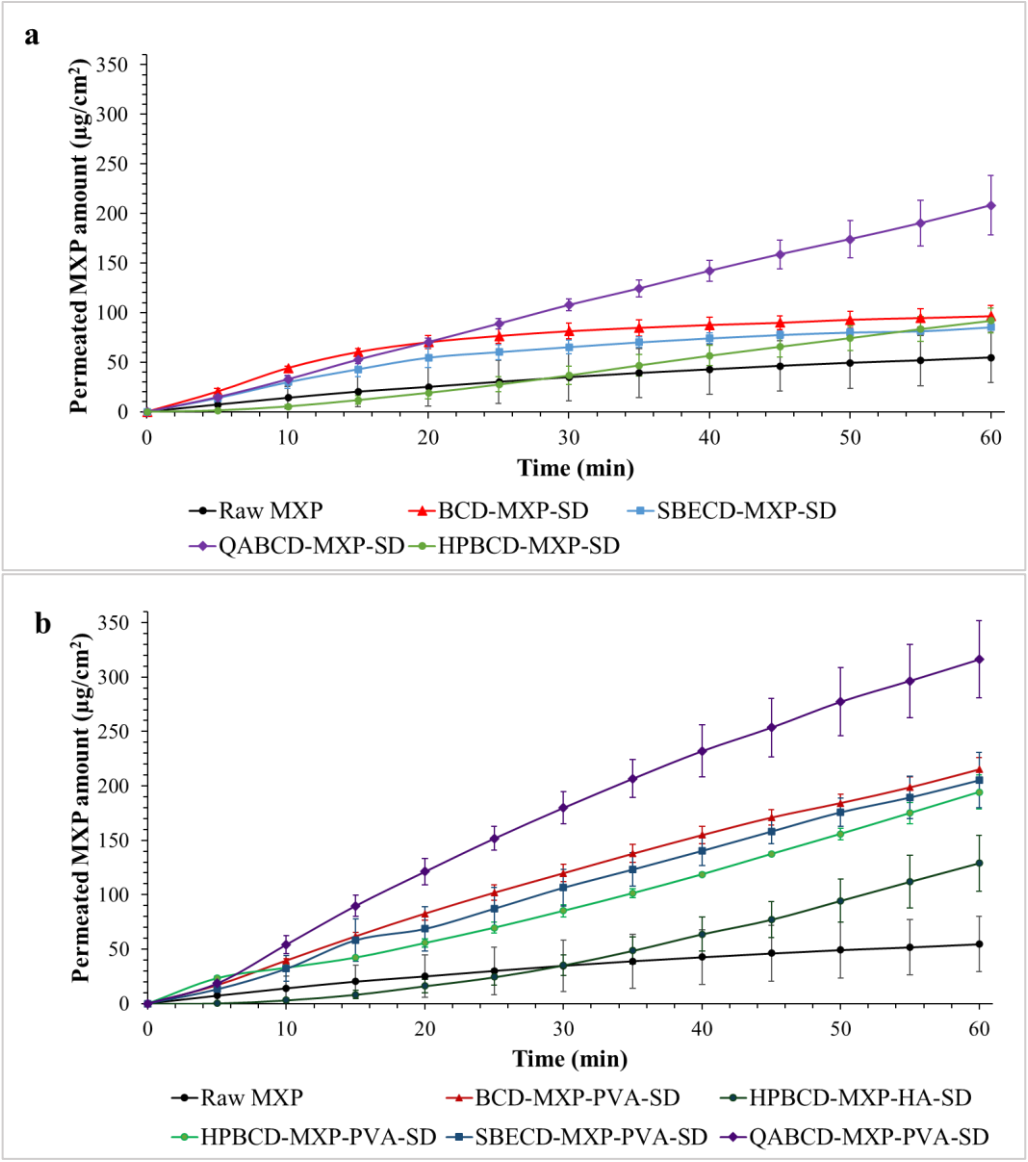

Figure 13. *In vitro* MXP diffusion from the (**a**) polymer-free and (**b**) polymer-containing formulations

5.3. Accelerated stability testing of the selected samples

5.3.1. Morphology of the spray-dried particles

The morphology was observed applying SEM, the images are shown in Figure 14. As stated before, spray drying resulted in spherical, smooth surfaced particles with an average particle size around 2 µm, this state of the powders was considered as a starting point. After 1 month of storage, differences in the morphology were detected. The BCD-based formulation did not show any obvious change, while aggregate formation between the particles of HPBCD-MXP-PVA-SD was clearly visible. The most drastic change in the morphology of the particles was

observed in the two charged CD-based formulations: the individual particles disappeared, merged, glass-like blocks were formed in both cases.

The exhibited changes were most likely a consequence of the highly humid environment, the charged CD-based formulations absorbed so much water, that they practically became liquified.

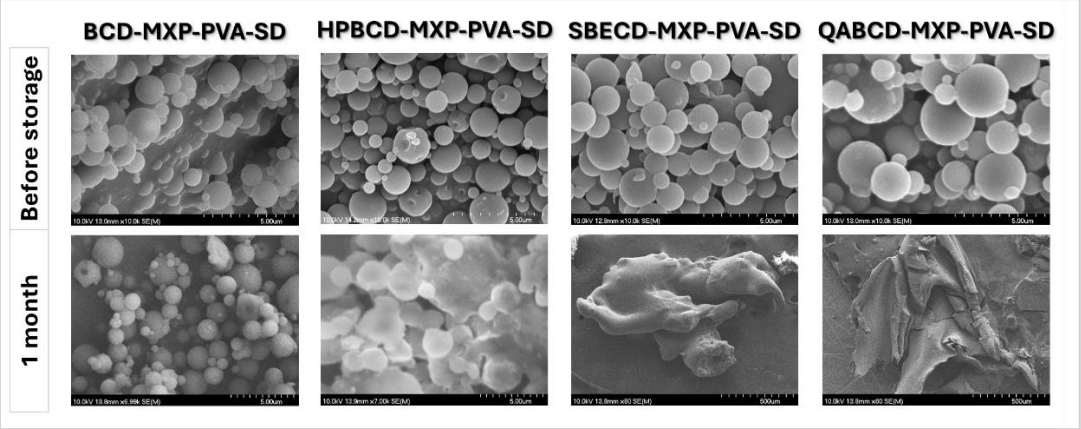

Figure 14. SEM images of the PVA-containing samples from before storage and after 1 month

5.3.2. Physico-chemical stability of the samples

The diffractograms of the samples put into stability are shown in Figure 15. As a result of spray drying, the initial formulations were amorphous, and after 1 month of storage, neither of the samples showed any signs of recrystallization. This could be attributed to both the presence of PVA and the amorphous CDs. Polymers and other originally amorphous matrices have a stabilizing effect on the amorphous structure of solid dispersions through the formation of H-bonds thereby reducing crystal nucleation and growth [149].

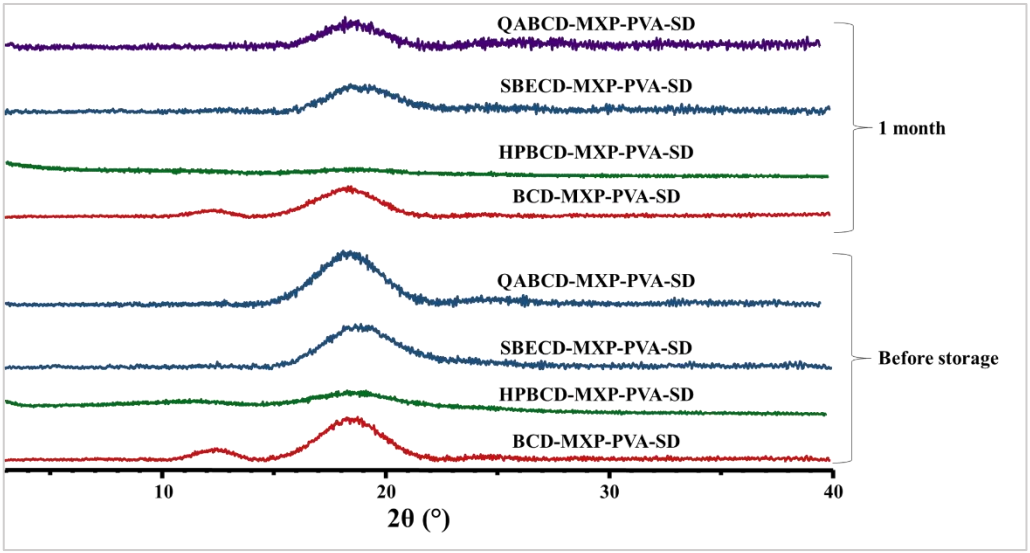

Figure 15. Diffractograms of the PVA-containing samples from before storage and after 1 month

The thermal behavior of the samples was also studied (Figure 16). Here it was found that the two neutral CD-based samples did not show any change in their thermograms, the formulations kept their amorphous structure, as detected by XRPD. However, new endothermic peaks appeared after 1 month in the thermograms of the SBECD- and QABCD-based samples. These were most likely present due to the water uptake of these formulations as it was visible in the SEM images.

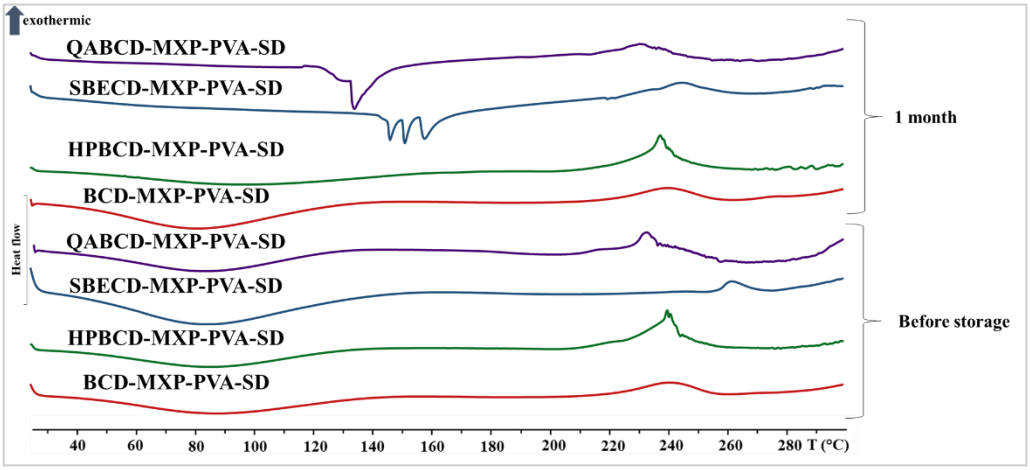

Figure 16. Thermograms of the PVA-containing samples from before storage and after 1 month

5.3.3. Drug content change in the samples

The drug content of the samples was also studied during the stability test, it is presented in Figure 17., the statistical comparison of the results was carried out with 2-sample t-tests. After 1 month, there was a significant decrease in the drug content of BCD-MXP-PVA-SD and

SBECD-MXP-PVA-SD sample comparing them to their “before storage” state. Their drug content was above the 5% acceptance limit defined by the ICH Q1A (R2) [150]. The experienced decrease was most likely due to the degradation of the API.

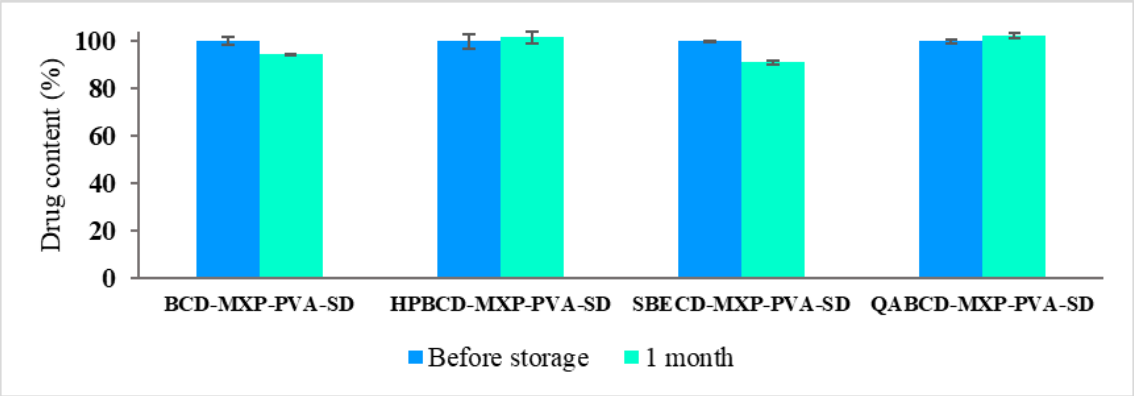

Figure 17. Drug content of the samples

5.3.4. Short discussion on the stability results

The accelerated stability test was carried out to have information on the physical, physico-chemical and chemical stability of the PVA-containing samples. Based on the results, it is not possible to select a “best” formulation in terms of stability, as the BCD-based sample showed the least change in morphology, all the samples kept their amorphous structure, and the drug content of HPBCD-based and QABCD-based samples did not change significantly. However, based on the findings of this study, it can be highlighted that the samples are sensitive to the humidity of the environment, which could be improved by further optimization of the composition and/or proper packaging.

In the next section, the cell-based experiments will be presented, for which the samples were selected based on the type of the CDs and the stability data.

5.4. Cell-based measurements

5.4.1. In vitro toxicity on RPMI 2650 cells

CDs and MXP alone as well as BCD-MXP-PVA-SD, SBECD-MXP-PVA-SD and QABCD-MXP-PVA-SD were selected for further cell-based measurements. Their non-toxic concentrations were determined based on their effects on membrane integrity and cell viability after 1 h of incubation using nasal RPMI 2650 cells.

As shown in Figure 18., CDs alone did not influence the cell viability, while they showed a concentration-dependent effect on the membrane integrity. BCD did not seem to disturb the membrane integrity in the tested concentration range, while SBECD and QABCD caused a

significant increase in the LDH release compared to cell control above 1 mM and 2.5 mM concentrations, respectively. According to our findings, BCD can be considered more tolerable to RPMI 2650 cells than QABCD and SBECD. The cytotoxic effect of these cyclodextrins had not been studied yet on RPMI 2650 cells except for BCD [151]. According to the literature, the toxicity of CDs correlates with their cholesterol extraction capacity [40]. In a study, QABCD and SBECD were found to be similarly safe at higher concentrations for the tested cells presenting similar cholesterol extraction capacity too, compared to other CDs [152]. It is important to emphasize that different cell types react to CDs to a different extent and the concentration and exposure time influence the results of the toxicity studies [153]. Too long exposure to high concentration CD solutions may lead to irreversible changes in the membranes leading to cell deaths, while lower concentrations with less exposure times can lead to reversely disturbed membrane integrity without notably decreasing cell viability [154].

Regarding raw MXP and the tested PVA-containing formulations, neither of them caused a significant increase in LDH release over the concentration range tested compared to the cell control. In contrast, cell viability assays indicated a significant decrease testing raw MXP solutions in the range of 125-25 μg/ml except for 25 μg/ml, but only the 125 μg/ml solution caused the viability to decrease to 68%. For the spray-dried formulations, only the 125 μg/ml MXP-containing solution of BCD-MXP-PVA-SD resulted in a significant reduction in viability to 72±2 %, neither SBECD-MXP-PVA-SD, nor QABCD-MXP-PVA-SD approached the viability threshold of 70 %, which is considered as non-toxic [155]. CDs can potentially play a protecting role against the toxic effect of APIs [156], which may have been the case here also, although other cell-based studies should be performed to prove this hypothesis.

For further experiment, to ensure that the results of the permeability study are not affected by the toxicity of the formulations so that the results are comparable, a concentration of 95 μg/ml of MXP was chosen as it was confirmed for every sample that it was not harmful to cells.

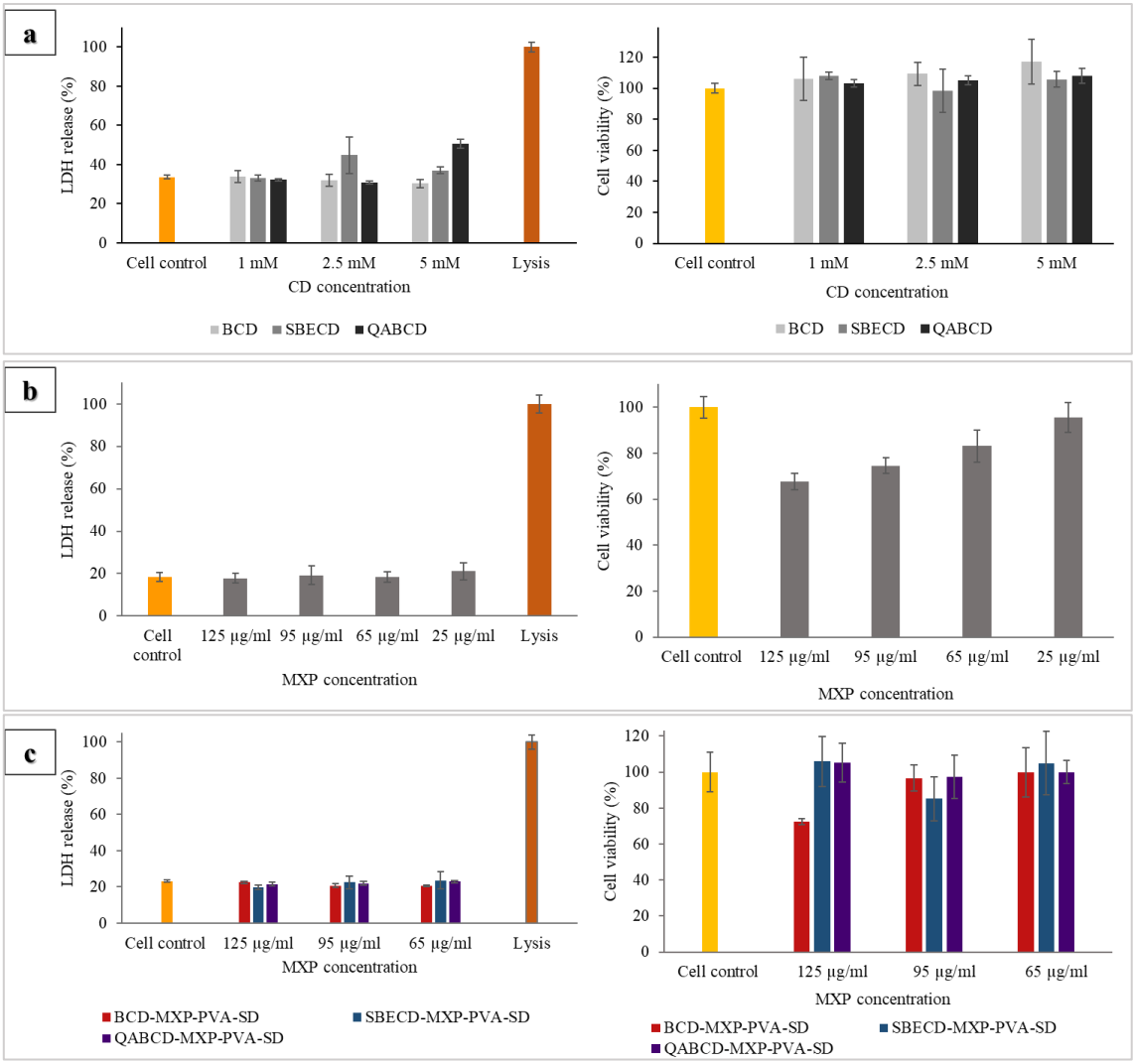

Figure 18. Effect on the LDH release and cell viability (%) of (**a**) CDs, (**b**) raw MXP and (**c**) the formulations

5.4.2. In vitro permeation studies applying RPMI 2650 nasal cells

For the permeation study, 95 µg/ml MXP concentration solutions were applied for the raw API as well as the PVA-containing formulations. The results are presented in Figure 19. and Table 6.

Among the samples, SBECD-MXP-PVA-SD exhibited a permeation of 4.5 µg/cm^2, which was significantly higher than all the other formulations and raw MXP, which showed comparable, lower permeation rates. After 60 mins, the highest drug concentration in the apical compartment was found for raw MXP. The QABCD-based and BCD-based samples demonstrated significant changes compared to raw MXP. SBECD-containing formulation resulted in the lowest drug concentration, significantly differing from all the other samples.

Taking into consideration both the permeation rate and the MXP-concentration in the apical compartment, it can be concluded that only the presence of the negatively charged

SBECD resulted in enhanced permeation of the drug on the tested cell line during the experimental period. CDs are known to have permeation enhancing features due to combined effects of two factors: improving the solubility of drugs making them accessible for absorption and interacting with biological membranes. In our case, the solubility enhancing effect of SBECD was not proven, most likely due to electrostatic repulsive forces between the negatively charged CD and meloxicam anion. However, SBECD could still have affected the cells, which proves that the presence of CDs may be favorable not only for drugs with low water-solubility. The comparison of our results with previous studies is difficult as there is only one study in the literature that involved RPMI 2650 nasal cells, mostly Caco-2 cells or excised mucosal tissues are applied for such studies [50,157]. Rassu et al. tested QABCD among others and reported the internalization of this CD in the RPMI 2650 cells making it potentially applicable for nasal administration of drugs [158]. In our case, the presence of this cationic CD was not proven to be favorable.

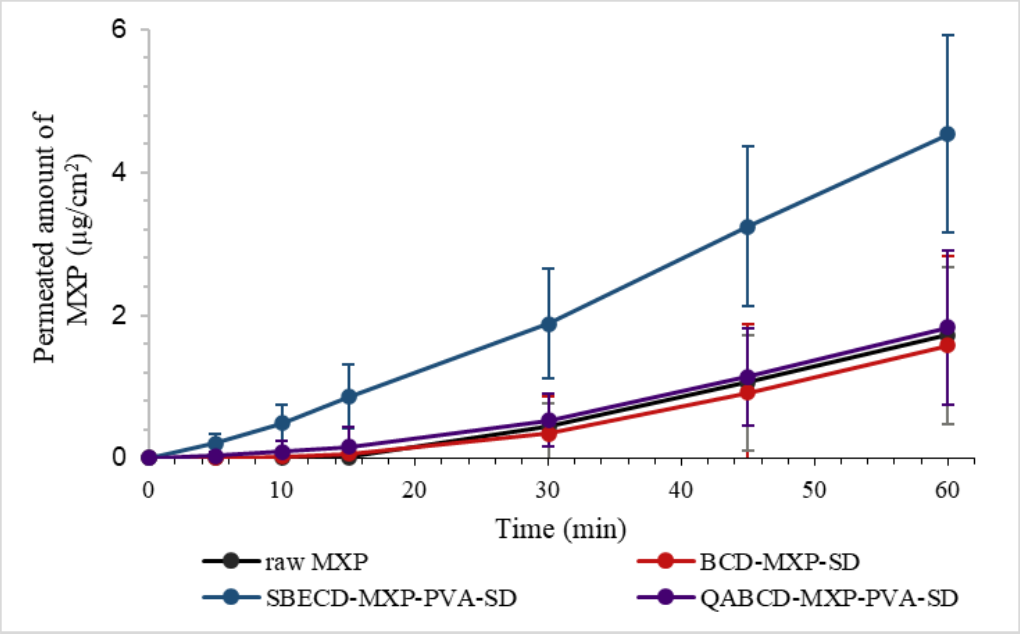

Figure 19. Permeated amount of MXP through RPMI 2650 cells

Table 6. MXP amount in the apical and basolateral compartment after 1 hour

	MXP amount in apical compartment after 60 min (%)	Permeated MXP amount after 60 min (%)
Raw MXP	79.6 ± 1.2	5.4 ± 2.9
BCD-MXP-PVA-SD	71.5 ± 1.0	5.5 ± 3.8
SBECD-MXP-PVA-SD	63.3 ± 0.6	15.8 ± 4.8
QABCD-MXP-PVA-SD	74.7 ± 4.8	6.4 ± 3.7

6. CONCLUSIONS

The findings of this PhD work, which aimed to prepare MXP-containing solid nasal dosage forms are summarized in the following points:

I. Based on the literature review, we decided to apply different beta-CDs and water-soluble polymers as they appeared to be promising excipient options to tackle the challenges this administration route faces: the relatively low permeability and the quick clearance of the administered drugs. Of all the preparation procedure options for nasal powders, nano spray drying was selected as it provides an opportunity to prepare particles with controlled size and morphology from liquid feed in a fast and easily scalable way. During our work, nasal powders were aimed to be prepared containing a patented but so far not marketed NSAID, MXP with a fast drug release (<5 min), good adhesion, physical and chemical stability and improved permeability. Up until now, the administration of NSAIDs through the nasal route for systemic action has been a less discovered area, only one NSAID-containing nasal spray is available on the market. Furthermore, only a few nasal powders have been marketed so far, which together with the lack of nasal pain relief options with NSAIDs justifies the relevancy of the topic selection of this Ph.D. work.

II. With the applied preparation method, microparticles were prepared with spherical morphology and smooth surface characteristics thanks to the lower drying rate. The originally crystalline materials, including MXP, were amorphized as a consequence of the preparation method in every sample which was confirmed by the XRPD and DSC measurements. In addition to that, the formation of secondary interactions between the CDs and MXP was confirmed except for the QABCD-based samples; however, the possibly formed electrostatic interaction between meloxicam anion and cationic QABCD was not detectable with the applied characterization method.

III. During the *in vitro* mucoadhesion test, the following phenomena were observed: (1) The maximum detachment force – which refers to the formed secondary interactions between the tested materials and mucin – was significantly higher in every case, except for BCD, than it was measured for raw MXP and mucin. This suggests that the presence of CDs contributed to the formation of these secondary interactions between the samples and mucin. (2) The powders presented comparably strong adhesion to a mucoadhesive chitosan derivative regardless of the presence of mucin which could have occurred due

to the dehydrating effect of the samples resulting in a strong physical interaction. This predicts the strong adhesion of all powders at their application site until their dissolution. (3) The type of CDs did not seem to affect the adhesion of the formulations based on this measurement. (4) Neither the formed secondary interactions, nor the strength of the adhesion was influenced by the presence of the polymers evidently. Although, this does not mean that the application of PVA and HA would not make sense, because the applied method was not able to detect the potential viscosity increasing effect of these polymers at the site of nasal powder application.

The *in vitro* dissolution of MXP under nasal conditions was accelerated significantly. The complete release of the API was observed in 1 min from all the samples compared to raw MXP which yielded only 46% in 5 min. This could be attributed to the formation of amorphous solid dispersions and the low particle size along with the presence of the highly water-soluble CDs. There was no difference observed based on the type of the CD or the applied polymer. The combination of this preparation method with the applied excipients can be considered highly suitable to prepare nasal powders with fast drug release.

The drug release was not a rate determining step in the *in vitro* permeation of MXP through the artificial mucosa. Here it was found that the type of the CD as well as the type of the polymer influenced the permeation rate. The cationic QABCD outperformed all the other samples in the presence of PVA. Even without PVA, it exhibited a similar permeation rate to the other, PVA-containing samples. It is hypothesized that the observed higher diffusion may be in connection with the presumably formed electrostatic attracting forces between meloxicam anion and cationic QABCD. Regarding the other polymer, HA also improved the permeation rate of MXP. Although, it significantly underperformed PVA, PVA improved the passive diffusion of MXP from all samples. As its positive effect was convincing, only PVA-containing samples were selected for further stability studies.

IV. The accelerated stability screening provided mixed results and conclusions; the choice of the best performing formulation was not possible. In terms of morphology, BCD-MXP-PVA-SD provided the best results, it maintained its morphology, the individual particles stayed noticeable, while all other formulation underwent significant morphological changes, which can be a major issue for powders. The amorphous state was maintained for all samples, the solid dispersion was stabilized by PVA and the amorphous CDs, while a decrease in drug content was detected for BCD- and SBECD-

based samples. The observed changes can be attributed to the effect of the conditions of the study, the high tendency to absorb water was proven for all the substituted CD-based samples. Cell-based measurements were proceeded with BCD-MXP-PVA-SD, SBECD-MXP-PVA-SD and QABCD-MXP-PVA-SD formulations.

V. The toxicity studies, which were carried out for the first time with the charged CDs and MXP on RPMI 2650 cells, revealed that while CDs affected the LDH release of the cells, MXP impacted the cell viability in a concentration dependent manner. BCD did not cause any significant change in the LDH release compared it to the cell control in the examined concentration range, while the 2.5 mM concentration of SBECD and 5 mM concentration of QABCD resulted in a significant increase. For raw MXP, the cell viability percentage was lower than 70% for the 125 μg/ml concentration solution which is considered as the acceptance limit of non-cytotoxic effect.

   The formulations were tested based on the MXP concentration of their solutions. Only the 125 μg/ml MXP concentration solution of BCD-MXP-PVA-SD caused a significant decrease in cell viability to 72%, all the other formulations exhibited higher viability values, which suggests that the applied CDs might have had a protecting effect on the cells at higher MXP concentrations. To ensure that the further permeation study results were not affected by the toxicity of the formulations, the 95 μg/ml MXP concentration-solutions were tested.

VI. For the permeation study of MXP, ALI-cultured RPMI 2650 cells were applied first in the literature to examine the potential permeation enhancing effect of the applied BCDs in nasal conditions. The accelerating effect of the CDs was evaluated taking into consideration the MXP amount in both the apical and the basolateral compartment. Based on that, it could be concluded that only SBECD had a significant impact on the diffusion of the API, which contrasted with the permeation results across the artificial mucosa. We hypothesize that MXP might not primarily be absorbed through passive diffusion and the CDs might have had a different effect on the cell membrane integrity and the tight junctions. This observation suggests the usefulness of this CD in improving the permeation of water-soluble drug.

VII. Lastly, to summarize the findings briefly, our preparation process yielded amorphous solid dispersions. The CDs – regardless of their type – contributed to the fast dissolution of the API together with the low particle size and the amorphous structure. Secondary interactions were detected with MXP in the formulations except for QABCD which may have formed electrostatic interaction with the drug. CDs also seemed to contribute to

the formation of secondary interactions with mucin in the mucoadhesion test, but the importance of their type was not confirmed evidently, for instance, the effect of their charge wasn't observed. The permeation of the API through an artificial mucosa examining the polymer-free samples was improved only in the presence of QABCD, the other CDs did not show a significant effect. In terms of stability, it was clearly visible that the highly water-soluble BCD derivatives tended to absorb the humidity of the environment due to which they could not maintain their morphology. Furthermore, the drug content of the SBECD- and BCD-based samples significantly decreased. The tolerability of the CDs to RPMI 2650 cells followed the order of BCD – 5 mM > QABCD – 2.5 mM > SBECD – 1 mM. The permeation enhancing effect on the cells for MXP was confirmed only for SBECD.

Regarding the applicability of polymers, neither PVA, nor HA had a proven effect on the rate of MXP dissolution or the adhesion of the samples. However, PVA exhibited convincing evidence for its permeation accelerating impact through the artificial mucosa, it significantly improved the drug diffusion in all cases. HA also improved drug diffusion, but its effect was significantly lower than PVA's. PVA most probably also contributed to maintaining the amorphous structure of the samples through the stability study.

The combination of BCDs and water-soluble polymers in nasal powder formulations for the absorption enhancement of MXP was reported first in the literature as a part of this Ph.D. work. Furthermore, the investigation of concentration-dependent cytotoxic effects of SBECD, QABCD, MXP and the mentioned formulations on RPMI 2650 nasal cell line had not been observed before. In addition to that, the permeation testing of MXP in the presence of the different BCDs and PVA was carried out first in the literature on ALI-cultured RPMI 2650 nasal cell line. Although SBECD-MXP-PVA-SD wasn't the best performing formulation in terms of drug diffusion through the artificial membrane or stability, the enhanced permeation of MXP through the nasal cell line was observed only for this sample. The combination of SBECD and PVA provides a good base for a novel nasal powder formulation with fast MXP release and potentially improved bioavailability. However, further optimization of the composition and the application of non-permeable packaging would be required to solve the stability issue.

REFERENCES

1. Kim, D.; Kim, Y.H.; Kwon, S. Enhanced Nasal Drug Delivery Efficiency by Increasing Mechanical Loading Using Hypergravity. *Sci. Rep.* **2018**, *8*, 168, doi:10.1038/s41598-017-18561-x.
2. Munkholm, M.; Mortensen, J. Mucociliary Clearance: Pathophysiological Aspects. *Clin. Physiol. Funct. Imaging* **2014**, *34*, 171–177, doi:10.1111/cpf.12085.
3. Szente, L. Highly Soluble Cyclodextrin Derivatives: Chemistry, Properties, and Trends in Development. *Adv. Drug Deliv. Rev.* **1999**, *36*, 17–28, doi:10.1016/S0169-409X(98)00092-1.
4. Lemmer, H.J.; Hamman, J.H. Paracellular Drug Absorption Enhancement through Tight Junction Modulation. *Expert Opin. Drug Deliv.* **2013**, *10*, 103–114, doi:10.1517/17425247.2013.745509.
5. Julinová, M.; Vaňharová, L.; Jurča, M. Water-Soluble Polymeric Xenobiotics – Polyvinyl Alcohol and Polyvinylpyrrolidon – And Potential Solutions to Environmental Issues: A Brief Review. *J. Environ. Manage.* **2018**, *228*, 213–222, doi:10.1016/j.jenvman.2018.09.010.
6. Trenkel, M.; Scherließ, R. Nasal Powder Formulations: In-Vitro Characterisation of the Impact of Powders on Nasal Residence Time and Sensory Effects. *Pharmaceutics* **2021**, *13*, 385, doi:10.3390/pharmaceutics13030385.
7. Cyriac, J.M.; James, E. Switch over from Intravenous to Oral Therapy: A Concise Overview. *J. Pharmacol. Pharmacother.* **2014**, *5*, 83–87, doi:10.4103/0976-500X.130042.
8. Gibaldi, M.; Boyes, R.N.; Feldman, S. Influence of First-Pass Effect on Availability of Drugs on Oral Administration. *J. Pharm. Sci.* **1971**, *60*, 1338–1340, doi:10.1002/jps.2600600909.
9. Gizurarson, S. The Relevance of Nasal Physiology to the Design of Drug Absorption Studies. *Adv. Drug Deliv. Rev.* **1993**, *11*, 329–347, doi:10.1016/0169-409X(93)90015-V.
10. Laffleur, F.; Bauer, B. Progress in Nasal Drug Delivery Systems. *Int. J. Pharm.* **2021**, *607*, 120994, doi:10.1016/j.ijpharm.2021.120994.
11. Illum, L. Nasal Drug Delivery—Possibilities, Problems and Solutions. *J. Controlled Release* **2003**, *87*, 187–198, doi:10.1016/S0168-3659(02)00363-2.
12. Arora, P.; Sharma, S.; Garg, S. Permeability Issues in Nasal Drug Delivery. *Drug Discov. Today* **2002**, *7*, 967–975, doi:10.1016/S1359-6446(02)02452-2.
13. Behl, C.R.; Pimplaskar, H.K.; Sileno, A.P.; deMeireles, J.; Romeo, V.D. Effects of Physicochemical Properties and Other Factors on Systemic Nasal Drug Delivery. *Adv. Drug Deliv. Rev.* **1998**, *29*, 89–116, doi:10.1016/S0169-409X(97)00063-X.
14. Mygind, N.; Dahl, R. Anatomy, Physiology and Function of the Nasal Cavities in Health and Disease. *Adv. Drug Deliv. Rev.* **1998**, *29*, 3–12, doi:10.1016/S0169-409X(97)00058-6.
15. Elad, D.; Wolf, M.; Keck, T. Air-Conditioning in the Human Nasal Cavity. *Respir. Physiol. Neurobiol.* **2008**, *163*, 121–127, doi:10.1016/j.resp.2008.05.002.
16. Stockhorst, U.; Pietrowsky, R. Olfactory Perception, Communication, and the Nose-to-Brain Pathway. *Physiol. Behav.* **2004**, *83*, 3–11, doi:10.1016/S0031-9384(04)00343-9.

17. Alberto, M.; Paiva-Santos, A.C.; Veiga, F.; Pires, P.C. Lipid and Polymeric Nanoparticles: Successful Strategies for Nose-to-Brain Drug Delivery in the Treatment of Depression and Anxiety Disorders. *Pharmaceutics* **2022**, *14*, 2742, doi:10.3390/pharmaceutics14122742.
18. Djupesland, P.G. Nasal Drug Delivery Devices: Characteristics and Performance in a Clinical Perspective—a Review. *Drug Deliv. Transl. Res.* **2013**, *3*, 42–62, doi:10.1007/s13346-012-0108-9.
19. Illum, L. Is Nose-to-Brain Transport of Drugs in Man a Reality? *J. Pharm. Pharmacol.* **2004**, *56*, 3–17, doi:10.1211/0022357022539.
20. Bitter, C.; Suter-Zimmermann, K.; Surber, C. Nasal Drug Delivery in Humans. In *Current Problems in Dermatology*; Surber, C., Elsner, P., Farage, M.A., Eds.; S. Karger AG, 2011; Vol. 40, pp. 20–35 ISBN 978-3-8055-9615-2.
21. Marttin, E.; Schipper, N.G.M.; Verhoef, J.C.; Merkus, F.W.H.M. Nasal Mucociliary Clearance as a Factor in Nasal Drug Delivery. *Adv. Drug Deliv. Rev.* **1998**, *29*, 13–38, doi:10.1016/S0169-409X(97)00059-8.
22. McShane, A.; Bath, J.; Jaramillo, A.M.; Ridley, C.; Walsh, A.A.; Evans, C.M.; Thornton, D.J.; Ribbeck, K. Mucus. *Curr. Biol.* **2021**, *31*, R938–R945, doi:10.1016/j.cub.2021.06.093.
23. Chung, S.; Peters, J.M.; Detyniecki, K.; Tatum, W.; Rabinowicz, A.L.; Carrazana, E. The Nose Has It: Opportunities and Challenges for Intranasal Drug Administration for Neurologic Conditions Including Seizure Clusters. *Epilepsy Behav. Rep.* **2023**, *21*, 100581, doi:10.1016/j.ebr.2022.100581.
24. Chaturvedi, M.; Kumar, M.; Pathak, K. A Review on Mucoadhesive Polymer Used in Nasal Drug Delivery System. *J. Adv. Pharm. Technol. Res.* **2011**, *2*, 215, doi:10.4103/2231-4040.90876.
25. Fortuna, A.; Alves, G.; Serralheiro, A.; Sousa, J.; Falcão, A. Intranasal Delivery of Systemic-Acting Drugs: Small-Molecules and Biomacromolecules. *Eur. J. Pharm. Biopharm.* **2014**, *88*, 8–27, doi:10.1016/j.ejpb.2014.03.004.
26. Collado-González, M.; González Espinosa, Y.; Goycoolea, F.M. Interaction Between Chitosan and Mucin: Fundamentals and Applications. *Biomimetics* **2019**, *4*, 32, doi:10.3390/biomimetics4020032.
27. Beule, A.G. Physiology and Pathophysiology of Respiratory Mucosa of the Nose and the Paranasal Sinuses. *GMS Curr. Top. Otorhinolaryngol. - Head Neck Surg. 9Doc07 ISSN 1865-1011* **2010**, doi:10.3205/CTO000071.
28. Nguyen, L.T.-T.; Duong, V.-A. Nose-to-Brain Drug Delivery. *Encyclopedia* **2025**, *5*, 91, doi:10.3390/encyclopedia5030091.
29. Kirtsreesakul, V.; Somjareonwattana, P.; Ruttanaphol, S. The Correlation between Nasal Symptom and Mucociliary Clearance in Allergic Rhinitis. *The Laryngoscope* **2009**, *119*, 1458–1462, doi:10.1002/lary.20146.
30. Mikolajczyk, M.; Janukowicz, K.; Majewska, E.; Baj, Z. Impact of Allergic Rhinitis on Nasal Mucociliary Clearance Time in Children. *Int. Arch. Allergy Immunol.* **2019**, *179*, 297–303, doi:10.1159/000499740.
31. Trenkel, M.; Scherließ, R. Optimising Nasal Powder Drug Delivery – Characterisation of the Effect of Excipients on Drug Absorption. *Int. J. Pharm.* **2023**, *633*, 122630, doi:10.1016/j.ijpharm.2023.122630.
32. Behl, C.R.; Pimplaskar, H.K.; Sileno, A.P.; Xia, W.J.; Gries, W.J.; deMeireles, J.C.; Romeo, V.D. Optimization of Systemic Nasal Drug Delivery with Pharmaceutical Excipients. *Adv. Drug Deliv. Rev.* **1998**, *29*, 117–133, doi:10.1016/S0169-409X(97)00064-1.

33. Ghadiri, M.; Young, P.M.; Traini, D. Strategies to Enhance Drug Absorption via Nasal and Pulmonary Routes. *Pharmaceutics* **2019**, *11*, 113, doi:10.3390/pharmaceutics11030113.
34. Davis, S.S.; Illum, L. Absorption Enhancers for Nasal Drug Delivery: *Clin. Pharmacokinet.* **2003**, *42*, 1107–1128, doi:10.2165/00003088-200342130-00003.
35. Hoang, V.D.; Uchenna, A.R.; Mark, J.; Renaat, K.; Norbert, V. Characterization of Human Nasal Primary Culture Systems to Investigate Peptide Metabolism. *Int. J. Pharm.* **2002**, *238*, 247–256, doi:10.1016/S0378-5173(02)00077-7.
36. Del Valle, E.M.M. Cyclodextrins and Their Uses: A Review. *Process Biochem.* **2004**, *39*, 1033–1046, doi:10.1016/S0032-9592(03)00258-9.
37. Jansook, P.; Ogawa, N.; Loftsson, T. Cyclodextrins: Structure, Physicochemical Properties and Pharmaceutical Applications. *Int. J. Pharm.* **2018**, *535*, 272–284, doi:10.1016/j.ijpharm.2017.11.018.
38. Davis, M.E.; Brewster, M.E. Cyclodextrin-Based Pharmaceutics: Past, Present and Future. *Nat. Rev. Drug Discov.* **2004**, *3*, 1023–1035, doi:10.1038/nrd1576.
39. Szejtli, J. Introduction and General Overview of Cyclodextrin Chemistry. *Chem. Rev.* **1998**, *98*, 1743–1754, doi:10.1021/cr970022c.
40. Kiss, T.; Fenyvesi, F.; Bácskay, I.; Váradi, J.; Fenyvesi, É.; Iványi, R.; Szente, L.; Tósaki, Á.; Vecsernyés, M. Evaluation of the Cytotoxicity of β-Cyclodextrin Derivatives: Evidence for the Role of Cholesterol Extraction. *Eur. J. Pharm. Sci.* **2010**, *40*, 376–380, doi:10.1016/j.ejps.2010.04.014.
41. Puskás, I.; Szente, L.; Szőcs, L.; Fenyvesi, É. Recent List of Cyclodextrin-Containing Drug Products. *Period. Polytech. Chem. Eng.* **2023**, *67*, 11–17, doi:10.3311/PPch.21222.
42. Ory, D.S.; Ottinger, E.A.; Farhat, N.Y.; King, K.A.; Jiang, X.; Weissfeld, L.; Berry-Kravis, E.; Davidson, C.D.; Bianconi, S.; Keener, L.A.; et al. Intrathecal 2-Hydroxypropyl-β-Cyclodextrin Decreases Neurological Disease Progression in Niemann-Pick Disease, Type C1: A Non-Randomised, Open-Label, Phase 1–2 Trial. *The Lancet* **2017**, *390*, 1758–1768, doi:10.1016/S0140-6736(17)31465-4.
43. Clemens, D.; Anderson, A.; Dinh, D.; Bhargava, P.; Sadrerafi, K.; Malanga, M.; Garcia-Fandiño, R.; Piñeiro, Á.; O'Connor, M. Reversing Atherosclerosis by the Specific Removal of Oxidized Cholesterol with Cyclodextrin Dimer. *Atherosclerosis* **2023**, *379*, S34–S35, doi:10.1016/j.atherosclerosis.2023.06.778.
44. Loftsson, T. Cyclodextrins and the Biopharmaceutics Classification System of Drugs. *J. Incl. Phenom. Macrocycl. Chem.* **2002**, *44*, 63–67, doi:10.1023/A:1023088423667.
45. Marttin, E.; Verhoef, J.C.; Merkus, F.W.H.M. Efficacy, Safety and Mechanism of Cyclodextrins as Absorption Enhancers in Nasal Delivery of Peptide and Protein Drugs. *J. Drug Target.* **1998**, *6*, 17–36, doi:10.3109/10611869808997878.
46. Hammoud, Z.; Khreich, N.; Auezova, L.; Fourmentin, S.; Elaissari, A.; Greige-Gerges, H. Cyclodextrin-Membrane Interaction in Drug Delivery and Membrane Structure Maintenance. *Int. J. Pharm.* **2019**, *564*, 59–76, doi:10.1016/j.ijpharm.2019.03.063.
47. Li, X.; Uehara, S.; Sawangrat, K.; Morishita, M.; Kusamori, K.; Katsumi, H.; Sakane, T.; Yamamoto, A. Improvement of Intestinal Absorption of Curcumin by Cyclodextrins and the Mechanisms Underlying Absorption Enhancement. *Int. J. Pharm.* **2018**, *535*, 340–349, doi:10.1016/j.ijpharm.2017.11.032.
48. Cheng, C.; Yuan, C.; Cui, B.; Lu, L.; Li, J.; Sha, H. Interfacial Behavior of Cyclodextrins at the Oil-Water Interface of Pickering Emulsion. *Food Hydrocoll.* **2023**, *134*, 108104, doi:10.1016/j.foodhyd.2022.108104.

49. Jagdale, S.K.; Dehghan, M.H.; Paul, N.S. Enhancement of Dissolution of Fenofibrate Using Complexation with Hydroxy Propyl β-Cyclodextrin. *Turk. J. Pharm. Sci.* **2019**, *16*, 48–53, doi:10.4274/tjps.60490.
50. Rassu, G.; Sorrenti, M.; Catenacci, L.; Pavan, B.; Ferraro, L.; Gavini, E.; Bonferoni, M.C.; Giunchedi, P.; Dalpiaz, A. Versatile Nasal Application of Cyclodextrins: Excipients and/or Actives? *Pharmaceutics* **2021**, *13*, 1180, doi:10.3390/pharmaceutics13081180.
51. Colombo, G.; Bortolotti, F.; Chiapponi, V.; Buttini, F.; Sonvico, F.; Invernizzi, R.; Quaglia, F.; Danesino, C.; Pagella, F.; Russo, P.; et al. Nasal Powders of Thalidomide for Local Treatment of Nose Bleeding in Persons Affected by Hereditary Hemorrhagic Telangiectasia. *Int. J. Pharm.* **2016**, *514*, 229–237, doi:10.1016/j.ijpharm.2016.07.002.
52. Tas, C.; Ozkan, C.K.; Savaser, A.; Ozkan, Y.; Tasdemir, U.; Altunay, H. Nasal Administration of Metoclopramide from Different Dosage Forms: In Vitro, Ex Vivo, and in Vivo Evaluation. *Drug Deliv.* **2009**, *16*, 167–175, doi:10.1080/10717540902764172.
53. Haschke, M.; Suter, K.; Hofmann, S.; Witschi, R.; Fröhlich, J.; Imanidis, G.; Drewe, J.; Briellmann, T.A.; Dussy, F.E.; Krähenbühl, S.; et al. Pharmacokinetics and Pharmacodynamics of Nasally Delivered Midazolam. *Br. J. Clin. Pharmacol.* **2010**, *69*, 607–616, doi:10.1111/j.1365-2125.2010.03611.x.
54. Yang, P.; Li, Y.; Li, W.; Zhang, H.; Gao, J.; Sun, J.; Yin, X.; Zheng, A. Preparation and Evaluation of Carfentanil Nasal Spray Employing Cyclodextrin Inclusion Technology. *Drug Dev. Ind. Pharm.* **2018**, *44*, 953–960, doi:10.1080/03639045.2018.1425426.
55. Babu, R.J.; Dayal, P.; Singh, M. Effect of Cyclodextrins on the Complexation and Nasal Permeation of Melatonin. *Drug Deliv.* **2008**, *15*, 381–388, doi:10.1080/10717540802006922.
56. Venuti, V.; Crupi, V.; Fazio, B.; Majolino, D.; Acri, G.; Testagrossa, B.; Stancanelli, R.; De Gaetano, F.; Gagliardi, A.; Paolino, D.; et al. Physicochemical Characterization and Antioxidant Activity Evaluation of Idebenone/Hydroxypropyl-β-Cyclodextrin Inclusion Complex †. *Biomolecules* **2019**, *9*, 531, doi:10.3390/biom9100531.
57. Luppi, B.; Bigucci, F.; Corace, G.; Delucca, A.; Cerchiara, T.; Sorrenti, M.; Catenacci, L.; Di Pietra, A.M.; Zecchi, V. Albumin Nanoparticles Carrying Cyclodextrins for Nasal Delivery of the Anti-Alzheimer Drug Tacrine. *Eur. J. Pharm. Sci.* **2011**, *44*, 559–565, doi:10.1016/j.ejps.2011.10.002.
58. Rassu, G.; Soddu, E.; Cossu, M.; Brundu, A.; Cerri, G.; Marchetti, N.; Ferraro, L.; Regan, R.F.; Giunchedi, P.; Gavini, E.; et al. Solid Microparticles Based on Chitosan or Methyl-β-Cyclodextrin: A First Formulative Approach to Increase the Nose-to-Brain Transport of Deferoxamine Mesylate. *J. Controlled Release* **2015**, *201*, 68–77, doi:10.1016/j.jconrel.2015.01.025.
59. Kadajji, V.G.; Betageri, G.V. Water Soluble Polymers for Pharmaceutical Applications. *Polymers* **2011**, *3*, 1972–2009, doi:10.3390/polym3041972.
60. *Pharmaceutical Applications of Polymers for Drug Delivery*; Jones, D.S., Ed.; Rapra review reports 0889-3144; Rapra Technology Ltd: Shawbury, U.K, 2004; ISBN 978-1-85957-479-9.
61. Ulery, B.D.; Nair, L.S.; Laurencin, C.T. Biomedical Applications of Biodegradable Polymers. *J. Polym. Sci. Part B Polym. Phys.* **2011**, *49*, 832–864, doi:10.1002/polb.22259.
62. Loftsson, T.; Masson, M. The Effects of Water-Soluble Polymers on Cyclodextrins and Cyclodextrin Solubilization of Drugs. *J. Drug Deliv. Sci. Technol.* **2004**, *14*, 35–43, doi:10.1016/S1773-2247(04)50003-5.

63. Qian, L.; Cook, M.T.; Dreiss, C.A. In Situ Gels for Nasal Delivery: Formulation, Characterization and Applications. *Macromol. Mater. Eng.* **2025**, *310*, 2400356, doi:10.1002/mame.202400356.
64. Smart, J. The Basics and Underlying Mechanisms of Mucoadhesion. *Adv. Drug Deliv. Rev.* **2005**, *57*, 1556–1568, doi:10.1016/j.addr.2005.07.001.
65. Vasquez-Martínez, N.; Guillen, D.; Moreno-Mendieta, S.A.; Sanchez, S.; Rodríguez-Sanoja, R. The Role of Mucoadhesion and Mucopenetration in the Immune Response Induced by Polymer-Based Mucosal Adjuvants. *Polymers* **2023**, *15*, 1615, doi:10.3390/polym15071615.
66. Huang, Y.; Leobandung, W.; Foss, A.; Peppas, N.A. Molecular Aspects of Muco- and Bioadhesion: *J. Controlled Release* **2000**, *65*, 63–71, doi:10.1016/S0168-3659(99)00233-3.
67. Gandhi, R.B.; Robinson, J.R. Oral Cavity as a Site for Bioadhesive Drug Delivery. *Adv. Drug Deliv. Rev.* **1994**, *13*, 43–74, doi:10.1016/0169-409X(94)90026-4.
68. Lee, J.W.; Park, J.H.; Robinson, J.R. Bioadhesive-Based Dosage Forms: The Next Generation. *J. Pharm. Sci.* **2000**, *89*, 850–866, doi:10.1002/1520-6017(200007)89:7<850::AID-JPS2>3.0.CO;2-G.
69. Bandi, S.P.; Bhatnagar, S.; Venuganti, V.V.K. Advanced Materials for Drug Delivery across Mucosal Barriers. *Acta Biomater.* **2021**, *119*, 13–29, doi:10.1016/j.actbio.2020.10.031.
70. *Bioadhesive Drug Delivery Systems: Fundamentals, Novel Approaches, and Development*; Mathiowitz, E., Chickering, D.E., Lehr, C.-M., Eds.; Drugs and the pharmaceutical sciences; Dekker: New York, 1999; ISBN 978-0-8247-1995-1.
71. Dumitriu, S. *Polymeric Biomaterials*; Marcel Dekker Inc: Hoboken, 2001; ISBN 978-0-203-90467-1.
72. Huh, Y.; Cho, H.-J.; Yoon, I.-S.; Choi, M.-K.; Kim, J.S.; Oh, E.; Chung, S.-J.; Shim, C.-K.; Kim, D.-D. Preparation and Evaluation of Spray-Dried Hyaluronic Acid Microspheres for Intranasal Delivery of Fexofenadine Hydrochloride. *Eur. J. Pharm. Sci.* **2010**, *40*, 9–15, doi:10.1016/j.ejps.2010.02.002.
73. Liu, H.; Chen, Y.; Wang, H.; Luo, X.; Xie, D.; Ji, Q.; Tian, L. Efficacy of Hyaluronic Acid in the Treatment of Nasal Inflammatory Diseases: A Systematic Review and Meta-Analysis. *Front. Pharmacol.* **2024**, *15*, 1350063, doi:10.3389/fphar.2024.1350063.
74. Sogias, I.A.; Williams, A.C.; Khutoryanskiy, V.V. Why Is Chitosan Mucoadhesive? *Biomacromolecules* **2008**, *9*, 1837–1842, doi:10.1021/bm800276d.
75. Benediktsdóttir, B.E.; Baldursson, Ó.; Másson, M. Challenges in Evaluation of Chitosan and Trimethylated Chitosan (TMC) as Mucosal Permeation Enhancers: From Synthesis to in Vitro Application. *J. Controlled Release* **2014**, *173*, 18–31, doi:10.1016/j.jconrel.2013.10.022.
76. Zheng, B.; Liu, D.; Qin, X.; Zhang, D.; Zhang, P. Mucoadhesive-to-Mucopenetrating Nanoparticles for Mucosal Drug Delivery: A Mini Review. *Int. J. Nanomedicine* **2025**, *Volume 20*, 2241–2252, doi:10.2147/IJN.S505427.
77. Song, B.; Cho, C.-W. Applying Polyvinyl Alcohol to the Preparation of Various Nanoparticles. *J. Pharm. Investig.* **2024**, *54*, 249–266, doi:10.1007/s40005-023-00649-4.
78. Baker, M.I.; Walsh, S.P.; Schwartz, Z.; Boyan, B.D. A Review of Polyvinyl Alcohol and Its Uses in Cartilage and Orthopedic Applications. *J. Biomed. Mater. Res. B Appl. Biomater.* **2012**, *100B*, 1451–1457, doi:10.1002/jbm.b.32694.

79. Popov, A.; Enlow, E.; Bourassa, J.; Chen, H. Mucus-Penetrating Nanoparticles Made with “Mucoadhesive” Poly(Vinyl Alcohol). *Nanomedicine Nanotechnol. Biol. Med.* **2016**, *12*, 1863–1871, doi:10.1016/j.nano.2016.04.006.
80. Loftsson, T.; Brewster, M.E. Pharmaceutical Applications of Cyclodextrins. 1. Drug Solubilization and Stabilization. *J. Pharm. Sci.* **1996**, *85*, 1017–1025, doi:10.1021/js950534b.
81. Cirri, M.; Maestrelli, F.; Corti, G.; Furlanetto, S.; Mura, P. Simultaneous Effect of Cyclodextrin Complexation, pH, and Hydrophilic Polymers on Naproxen Solubilization. *J. Pharm. Biomed. Anal.* **2006**, *42*, 126–131, doi:10.1016/j.jpba.2005.11.029.
82. Ge, Y.; Xu, X.; Cao, M.; Liu, B.; Wang, Y.; Liao, P.; Wang, J.; Chen, Y.; Yuan, H.; Chen, G. Nasal Drug Delivery and Nose-to-Brain Delivery Technology Development Status and Trend Analysis: Based on Questionnaire Survey and Patent Analysis. *Pharmaceutics* **2024**, *16*, 929, doi:10.3390/pharmaceutics16070929.
83. Tai, J.; Han, M.; Lee, D.; Park, I.-H.; Lee, S.H.; Kim, T.H. Different Methods and Formulations of Drugs and Vaccines for Nasal Administration. *Pharmaceutics* **2022**, *14*, 1073, doi:10.3390/pharmaceutics14051073.
84. Baldelli, A.; Boraey, M.A.; Oguzlu, H.; Cidem, A.; Rodriguez, A.P.; Ong, H.X.; Jiang, F.; Bacca, M.; Thamboo, A.; Traini, D.; et al. Engineered Nasal Dry Powder for the Encapsulation of Bioactive Compounds. *Drug Discov. Today* **2022**, *27*, 2300–2308, doi:10.1016/j.drudis.2022.04.012.
85. Bartos, C.; Pallagi, E.; Szabó-Révész, P.; Ambrus, R.; Katona, G.; Kiss, T.; Rahimi, M.; Csóka, I. Formulation of Levodopa Containing Dry Powder for Nasal Delivery Applying the Quality-by-Design Approach. *Eur. J. Pharm. Sci.* **2018**, *123*, 475–483, doi:10.1016/j.ejps.2018.07.061.
86. Tanaka, H.; Ochii, Y.; Moroto, Y.; Hirata, D.; Ibaraki, T.; Ogawara, K. Nanocrystal Preparation of Poorly Water-Soluble Drugs with Low Metal Contamination Using Optimized Bead-Milling Technology. *Pharmaceutics* **2022**, *14*, 2633, doi:10.3390/pharmaceutics14122633.
87. Preston, K.B.; Randolph, T.W. Stability of Lyophilized and Spray Dried Vaccine Formulations. *Adv. Drug Deliv. Rev.* **2021**, *171*, 50–61, doi:10.1016/j.addr.2021.01.016.
88. Dixit, M.; Kulkarni, P.K. Lyophilization Monophase Solution Technique for Improvement of the Solubility and Dissolution of Piroxicam. *Res. Pharm. Sci.* **2012**, *7*, 13–21.
89. Wang, W. Lyophilization and Development of Solid Protein Pharmaceuticals. *Int. J. Pharm.* **2000**, *203*, 1–60, doi:10.1016/S0378-5173(00)00423-3.
90. Barbosa, J.; Borges, S.; Amorim, M.; Pereira, M.J.; Oliveira, A.; Pintado, M.E.; Teixeira, P. Comparison of Spray Drying, Freeze Drying and Convective Hot Air Drying for the Production of a Probiotic Orange Powder. *J. Funct. Foods* **2015**, *17*, 340–351, doi:10.1016/j.jff.2015.06.001.
91. Seville, P.C.; Li, H.; Learoyd, T.P. Spray-Dried Powders for Pulmonary Drug Delivery. *Crit. Rev. Ther. Drug Carrier Syst.* **2007**, *24*, 307–360, doi:10.1615/CritRevTherDrugCarrierSyst.v24.i4.10.
92. Li, X.; Anton, N.; Arpagaus, C.; Belleteix, F.; Vandamme, T.F. Nanoparticles by Spray Drying Using Innovative New Technology: The Büchi Nano Spray Dryer B-90. *J. Controlled Release* **2010**, *147*, 304–310, doi:10.1016/j.jconrel.2010.07.113.

93. Homayoonfal, M.; Malekjani, N.; Baeghbali, V.; Ansarifar, E.; Hedayati, S.; Jafari, S.M. Optimization of Spray Drying Process Parameters for the Food Bioactive Ingredients. *Crit. Rev. Food Sci. Nutr.* **2024**, *64*, 5631–5671, doi:10.1080/10408398.2022.2156976.
94. Lebrun, P.; Krier, F.; Mantanus, J.; Grohganz, H.; Yang, M.; Rozet, E.; Boulanger, B.; Evrard, B.; Rantanen, J.; Hubert, P. Design Space Approach in the Optimization of the Spray-Drying Process. *Eur. J. Pharm. Biopharm.* **2012**, *80*, 226–234, doi:10.1016/j.ejpb.2011.09.014.
95. Gallo, L.; Verónica Ramírez-Rigo, M.; Bucalá, V. Development of Porous Spray-Dried Inhalable Particles Using an Organic Solvent-Free Technique. *Powder Technol.* **2019**, *342*, 642–652, doi:10.1016/j.powtec.2018.10.041.
96. Singh, A.; Van Den Mooter, G. Spray Drying Formulation of Amorphous Solid Dispersions. *Adv. Drug Deliv. Rev.* **2016**, *100*, 27–50, doi:10.1016/j.addr.2015.12.010.
97. Patil, S.; Babbar, A.; Mathur, R.; Mishra, A.; Sawant, K. Mucoadhesive Chitosan Microspheres of Carvedilol for Nasal Administration. *J. Drug Target.* **2010**, *18*, 321–331, doi:10.3109/10611861003663523.
98. Zhao, Y.; Brown, M.B.; Khengar, R.H.; Traynor, M.J.; Barata, P.; Jones, S.A. Pharmacokinetic Evaluation of Intranasally Administered Vinyl Polymer-Coated Lorazepam Microparticles in Rabbits. *AAPS J.* **2012**, *14*, 218–224, doi:10.1208/s12248-012-9325-x.
99. Tatsuta, R.; Tanaka, A.; Ogawara, K.; Higaki, K.; Furubayashi, T.; Sakane, T. In Vivo Systemic Evaluation of Nasal Drug Absorption from Powder Formulations in Rats. *Eur. J. Pharm. Biopharm.* **2025**, *207*, 114612, doi:10.1016/j.ejpb.2024.114612.
100. Basaria, A.A.A.; Sah, S.; Ratnani, H.; Fatima, I.; Yokolo, H. Atzumi for Migraine a New Era of Needle-Free Dihydroergotamine Delivery. *Ann. Med. Surg.* **2025**, doi:10.1097/MS9.0000000000003652.
101. Baqsimi™ - Product Information.
102. Freitag, F.G.; Shumate, D.A. The Efficacy and Safety of Sumatriptan Intranasal Powder in Adults with Acute Migraine. *Expert Rev. Neurother.* **2016**, *16*, 743–747, doi:10.1080/14737175.2016.1195687.
103. Pozzoli, M.; Rogueda, P.; Zhu, B.; Smith, T.; Young, P.M.; Traini, D.; Sonvico, F. Dry Powder Nasal Drug Delivery: Challenges, Opportunities and a Study of the Commercial Teijin Puvlizer Rhinocort Device and Formulation. *Drug Dev. Ind. Pharm.* **2016**, *42*, 1660–1668, doi:10.3109/03639045.2016.1160110.
104. Smith, J.; Ng, L. The Management of Acute Pain – an Update. *Medicine (Baltimore)* **2025**, *53*, 102–108, doi:10.1016/j.mpmed.2024.11.007.
105. Engelhardt, G. Pharmacology of Meloxicam, A New Non-Steroidal Anti-Inflammatory Drug with an Improved Safety Profile Through Preferential Inhibition of COX-2. *Rheumatology* **1996**, *35*, 4–12, doi:10.1093/rheumatology/35.suppl_1.4.
106. Türck, D.; Busch, U.; Heinzel, G.; Narjes, H. Clinical Pharmacokinetics of Meloxicam. *Arzneimittelforschung.* **1997**, *47*, 253–258.
107. Parekh, V.J.; Desai, N.D.; Shaikh, M.S.; Shinde, U.A. Self Nanoemulsifying Granules (SNEGs) of Meloxicam: Preparation, Characterization, Molecular Modeling and Evaluation of *in Vivo* Anti-Inflammatory Activity. *Drug Dev. Ind. Pharm.* **2017**, *43*, 600–610, doi:10.1080/03639045.2016.1275665.
108. Mezei, T.; Simig, G.; Molnár, E.; Lukács, G.; Porcs-Makkay, M.; Volk, B.; Hofmanné Fekete, V.; Nagy, K.; Mesterházy, N.; Krasznai, G.; et al. Process for Preparation of High-Purity Meloxicam and Meloxicam Potassium Salt.

109. Chvatal, A.; Farkas, Á.; Balásházy, I.; Szabó-Révész, P.; Ambrus, R. Aerodynamic Properties and in Silico Deposition of Meloxicam Potassium Incorporated in a Carrier-Free DPI Pulmonary System. *Int. J. Pharm.* **2017**, *520*, 70–78, doi:10.1016/j.ijpharm.2017.01.070.
110. WHO Guidelines for the Pharmacological and Radiotherapeutic Management of Cancer Pain in Adults and Adolescents 2018.
111. Martinez, L.; Ekman, E.; Nakhla, N. Perioperative Opioid-Sparing Strategies: Utility of Conventional NSAIDs in Adults. *Clin. Ther.* **2019**, *41*, 2612–2628, doi:10.1016/j.clinthera.2019.10.002.
112. Finnerup, N.B.; Attal, N.; Haroutounian, S.; McNicol, E.; Baron, R.; Dworkin, R.H.; Gilron, I.; Haanpää, M.; Hansson, P.; Jensen, T.S.; et al. Pharmacotherapy for Neuropathic Pain in Adults: A Systematic Review and Meta-Analysis. *Lancet Neurol.* **2015**, *14*, 162–173, doi:10.1016/S1474-4422(14)70251-0.
113. Shin, J.H.; Choi, K.Y.; Kim, Y.C.; Lee, M.G. Dose-Dependent Pharmacokinetics of Itraconazole after Intravenous or Oral Administration to Rats: Intestinal First-Pass Effect. *Antimicrob. Agents Chemother.* **2004**, *48*, 1756–1762, doi:10.1128/AAC.48.5.1756-1762.2004.
114. Zhou, Q.; Jin, J.; Zhu, L.; Chen, M.; Xu, H.; Wang, H.; Feng, X.; Zhu, X. The Optimal Choice of Medication Administration Route Regarding Intravenous, Intramuscular, and Subcutaneous Injection. *Patient Prefer. Adherence* **2015**, 923, doi:10.2147/PPA.S87271.
115. Dale, O.; Hjortkjær, R.; Kharasch, E.D. Nasal Administration of Opioids for Pain Management in Adults. *Acta Anaesthesiol. Scand.* **2002**, *46*, 759–770, doi:10.1034/j.1399-6576.2002.460702.x.
116. Bacon, R.; Newman, S.; Rankin, L.; Pitcairn, G.; Whiting, R. Pulmonary and Nasal Deposition of Ketorolac Tromethamine Solution (SPRIX) Following Intranasal Administration. *Int. J. Pharm.* **2012**, *431*, 39–44, doi:10.1016/j.ijpharm.2012.04.023.
117. Nakhaee, S.; Saeedi, F.; Mehrpour, O. Clinical and Pharmacokinetics Overview of Intranasal Administration of Fentanyl. *Heliyon* **2023**, *9*, e23083, doi:10.1016/j.heliyon.2023.e23083.
118. Madani, M. Effectiveness of Stadol NS (Butorphanol Tartrate) with Ibuprofen in the Treatment of Pain after Laser-Assisted Uvulopalatopharyngoplasty. *J. Oral Maxillofac. Surg.* **2000**, *58*, 27–31, doi:10.1053/joms.2000.17881.
119. Martin, V.; Hoekman, J.; Aurora, S.K.; Shrewsbury, S.B. Nasal Delivery of Acute Medications for Migraine: The Upper Versus Lower Nasal Space. *J. Clin. Med.* **2021**, *10*, 2468, doi:10.3390/jcm10112468.
120. Rapoport, A.M.; Bigal, M.E.; Tepper, S.J.; Sheftell, F.D. Zolmitriptan (Zomig®). *Expert Rev. Neurother.* **2004**, *4*, 33–41, doi:10.1586/14737175.4.1.33.
121. Dafer, R.M.; Tietjen, G.E.; Rothrock, J.F.; Vann, R.E.; Shrewsbury, S.B.; Aurora, S.K. Cardiovascular Safety of Dihydroergotamine Mesylate Delivered by Precision Olfactory Delivery (INP104) for the Acute Treatment of Migraine. *Headache J. Head Face Pain* **2024**, *64*, 983–994, doi:10.1111/head.14669.
122. Dhillon, S. Zavegepant: First Approval. *Drugs* **2023**, *83*, 825–831, doi:10.1007/s40265-023-01885-6.
123. Saokham, P.; Muankaew, C.; Jansook, P.; Loftsson, T. Solubility of Cyclodextrins and Drug/Cyclodextrin Complexes. *Molecules* **2018**, *23*, 1161, doi:10.3390/molecules23051161.
124. Challa, R.; Ahuja, A.; Ali, J.; Khar, R.K. Cyclodextrins in Drug Delivery: An Updated Review. *AAPS PharmSciTech* **2005**, *6*, E329–E357, doi:10.1208/pt060243.
125. Loftsson, T.; Hreinsdóttir, D.; Másson, M. Evaluation of Cyclodextrin Solubilization of Drugs. *Int. J. Pharm.* **2005**, *302*, 18–28, doi:10.1016/j.ijpharm.2005.05.042.

126. Fenyvesi, F.; Nguyen, T.L.P.; Haimhoffer, Á.; Rusznyák, Á.; Vasvári, G.; Bácskay, I.; Vecsernyés, M.; Ignat, S.-R.; Dinescu, S.; Costache, M.; et al. Cyclodextrin Complexation Improves the Solubility and Caco-2 Permeability of Chrysin. *Materials* **2020**, *13*, 3618, doi:10.3390/ma13163618.
127. Poór, M.; Kunsági-Máté, S.; Szente, L.; Matisz, G.; Secenji, G.; Czibulya, Z.; Kőszegi, T. Interaction of Ochratoxin A with Quaternary Ammonium Beta-Cyclodextrin. *Food Chem.* **2015**, *172*, 143–149, doi:10.1016/j.foodchem.2014.09.034.
128. Gil, E.S.; Li, J.; Xiao, H.; Lowe, T.L. Quaternary Ammonium β-Cyclodextrin Nanoparticles for Enhancing Doxorubicin Permeability across the In Vitro Blood−Brain Barrier. *Biomacromolecules* **2009**, *10*, 505–516, doi:10.1021/bm801026k.
129. Horvát, S.; Fehér, A.; Wolburg, H.; Sipos, P.; Veszelka, S.; Tóth, A.; Kis, L.; Kurunczi, A.; Balogh, G.; Kürti, L.; et al. Sodium Hyaluronate as a Mucoadhesive Component in Nasal Formulation Enhances Delivery of Molecules to Brain Tissue. *Eur. J. Pharm. Biopharm.* **2009**, *72*, 252–259, doi:10.1016/j.ejpb.2008.10.009.
130. Peppas, N.A.; Mongia, N.K. Ultrapure Poly(Vinyl Alcohol) Hydrogels with Mucoadhesive Drug Delivery Characteristics. *Eur. J. Pharm. Biopharm.* **1997**, *43*, 51–58, doi:10.1016/S0939-6411(96)00010-0.
131. Nho, Y.-C.; Park, J.-S.; Lim, Y.-M. Preparation of Poly(Acrylic Acid) Hydrogel by Radiation Crosslinking and Its Application for Mucoadhesives. *Polymers* **2014**, *6*, 890–898, doi:10.3390/polym6030890.
132. Burgess, D.J.; Duffy, E.; Etzler, F.; Hickey, A.J. Particle Size Analysis: AAPS Workshop Report, Cosponsored by the Food and Drug Administration and the United States Pharmacopeia. *AAPS J.* **2004**, *6*, 23–34, doi:10.1208/aapsj060320.
133. Rigaut, C.; Deruyver, L.; Goole, J.; Haut, B.; Lambert, P. Instillation of a Dry Powder in Nasal Casts: Parameters Influencing the Olfactory Deposition With Uni- and Bi-Directional Devices. *Front. Med. Technol.* **2022**, *4*, 924501, doi:10.3389/fmedt.2022.924501.
134. Vehring, R. Pharmaceutical Particle Engineering via Spray Drying. *Pharm. Res.* **2008**, *25*, 999–1022, doi:10.1007/s11095-007-9475-1.
135. Almansour, K.; Ali, R.; Alheibshy, F.; Almutairi, T.J.; Alshammari, R.F.; Alhajj, N.; Arpagaus, C.; Elsayed, M.M.A. Particle Engineering by Nano Spray Drying: Optimization of Process Parameters with Hydroethanolic versus Aqueous Solutions. *Pharmaceutics* **2022**, *14*, 800, doi:10.3390/pharmaceutics14040800.
136. Borba, P.A.A.; Pinotti, M.; Andrade, G.R.S.; Da Costa, N.B.; Olchanheski, L.R.; Fernandes, D.; De Campos, C.E.M.; Stulzer, H.K. The Effect of Mechanical Grinding on the Formation, Crystalline Changes and Dissolution Behaviour of the Inclusion Complex of Telmisartan and β-Cyclodextrins. *Carbohydr. Polym.* **2015**, *133*, 373–383, doi:10.1016/j.carbpol.2015.06.098.
137. Tambe, S.; Jain, D.; Meruva, S.K.; Rongala, G.; Juluri, A.; Nihalani, G.; Mamidi, H.K.; Nukala, P.K.; Bolla, P.K. Recent Advances in Amorphous Solid Dispersions: Preformulation, Formulation Strategies, Technological Advancements and Characterization. *Pharmaceutics* **2022**, *14*, 2203, doi:10.3390/pharmaceutics14102203.
138. Zhang, J.; Guo, M.; Luo, M.; Cai, T. Advances in the Development of Amorphous Solid Dispersions: The Role of Polymeric Carriers. *Asian J. Pharm. Sci.* **2023**, *18*, 100834, doi:10.1016/j.ajps.2023.100834.

139. Mezei, T.; Mesterházy, N.; Bakó, T.; Porcs-Makkay, M.; Simig, G.; Volk, B. Manufacture of High-Purity Meloxicam via Its Novel Potassium Salt Monohydrate. *Org. Process Res. Dev.* **2009**, *13*, 567–572, doi:10.1021/op900031h.
140. Rodríguez-Tenreiro, C.; Alvarez-Lorenzo, C.; Concheiro, Á.; Torres-Labandeira, J.J. Characterization of Cyclodextrincarbopol Interactions by DSC and FTIR. *J. Therm. Anal. Calorim.* **2004**, *77*, 403–411, doi:10.1023/B:JTAN.0000038981.30494.f4.
141. Mahmoud, A.A.; El-Feky, G.S.; Kamel, R.; Awad, G.E.A. Chitosan/Sulfobutylether-β-Cyclodextrin Nanoparticles as a Potential Approach for Ocular Drug Delivery. *Int. J. Pharm.* **2011**, *413*, 229–236, doi:10.1016/j.ijpharm.2011.04.031.
142. Samra, M.M.; Sadia, A.; Azam, M.; Imran, M.; Ahmad, I.; Basra, M.A.R. Synthesis, Spectroscopic and Biological Investigation of a New Ca(II) Complex of Meloxicam as Potential COX-2 Inhibitor. *Arab. J. Sci. Eng.* **2022**, *47*, 7105–7122, doi:10.1007/s13369-021-06521-7.
143. Mohit, V.; Harshal, G.; Neha, D.; Vilasrao, K.; Rajashree, H. A Comparative Study of Complexation Methods for Cefdinir-Hydroxypropyl-β-Cyclodextrin System. *J. Incl. Phenom. Macrocycl. Chem.* **2011**, *71*, 57–66, doi:10.1007/s10847-010-9901-6.
144. Yuan, C.; Liu, B.; Liu, H. Characterization of Hydroxypropyl-β-Cyclodextrins with Different Substitution Patterns via FTIR, GC–MS, and TG–DTA. *Carbohydr. Polym.* **2015**, *118*, 36–40, doi:10.1016/j.carbpol.2014.10.070.
145. Bayat, F.; Homami, S.S.; Monzavi, A.; Olyai, M.R.T.B. Synthesis and Characterization of Ataluren-Cyclodextrins Complexes. *J. Mol. Struct.* **2023**, *1272*, 134053, doi:10.1016/j.molstruc.2022.134053.
146. Park, C.R.; Munday, D.L. Development and Evaluation of a Biphasic Buccal Adhesive Tablet for Nicotine Replacement Therapy. *Int. J. Pharm.* **2002**, *237*, 215–226, doi:10.1016/S0378-5173(02)00041-8.
147. Kiss, T.; Ambrus, R.; Abdelghafour, M.M.; Zeiringer, S.; Selmani, A.; Roblegg, E.; Budai-Szűcs, M.; Janovák, L.; Lőrinczi, B.; Deák, Á.; et al. Preparation and Detailed Characterization of the Thiomer Chitosan–Cysteine as a Suitable Mucoadhesive Excipient for Nasal Powders. *Int. J. Pharm.* **2022**, *626*, 122188, doi:10.1016/j.ijpharm.2022.122188.
148. Khadka, P.; Ro, J.; Kim, H.; Kim, I.; Kim, J.T.; Kim, H.; Cho, J.M.; Yun, G.; Lee, J. Pharmaceutical Particle Technologies: An Approach to Improve Drug Solubility, Dissolution and Bioavailability. *Asian J. Pharm. Sci.* **2014**, *9*, 304–316, doi:10.1016/j.ajps.2014.05.005.
149. Shi, Q.; Chen, H.; Wang, Y.; Wang, R.; Xu, J.; Zhang, C. Amorphous Solid Dispersions: Role of the Polymer and Its Importance in Physical Stability and In Vitro Performance. *Pharmaceutics* **2022**, *14*, 1747, doi:10.3390/pharmaceutics14081747.
150. STABILITY TESTING OF NEW DRUG SUBSTANCES AND PRODUCTS Q1A(R2).
151. Horváth, T.; Bartos, C.; Bocsik, A.; Kiss, L.; Veszelka, S.; Deli, M.; Újhelyi, G.; Szabó-Révész, P.; Ambrus, R. Cytotoxicity of Different Excipients on RPMI 2650 Human Nasal Epithelial Cells. *Molecules* **2016**, *21*, 658, doi:10.3390/molecules21050658.
152. Nehr-Majoros, A.K.; Erostyák, J.; Fenyvesi, É.; Szabó-Meleg, E.; Szőcs, L.; Sétáló, G.; Helyes, Z.; Szőke, É. Cyclodextrin Derivatives Decrease Transient Receptor Potential Vanilloid 1 and Ankyrin 1 Ion Channel Activation via Altering the Surrounding Membrane Microenvironment by Cholesterol Depletion. *Front. Cell Dev. Biol.* **2024**, *12*, 1334130, doi:10.3389/fcell.2024.1334130.

153. Trotta, F.; Loftsson, T.; Gaud, R.S.; Trivedi, R.; Shende, P. Integration of Cyclodextrins and Associated Toxicities: A Roadmap for High Quality Biomedical Applications. *Carbohydr. Polym.* **2022**, *295*, 119880, doi:10.1016/j.carbpol.2022.119880.
154. Musuc, A.M. Cyclodextrins: Advances in Chemistry, Toxicology, and Multifaceted Applications. *Molecules* **2024**, *29*, 5319, doi:10.3390/molecules29225319.
155. Tetyczka, C.; Griesbacher, M.; Absenger-Novak, M.; Fröhlich, E.; Roblegg, E. Development of Nanostructured Lipid Carriers for Intraoral Delivery of Domperidone. *Int. J. Pharm.* **2017**, *526*, 188–198, doi:10.1016/j.ijpharm.2017.04.076.
156. Mantik, P.; Xie, M.; Wong, H.; La, H.; Steigerwalt, R.W.; Devanaboyina, U.; Ganem, G.; Shih, D.; Flygare, J.A.; Fairbrother, W.J.; et al. Cyclodextrin Reduces Intravenous Toxicity of a Model Compound. *J. Pharm. Sci.* **2019**, *108*, 1934–1943, doi:10.1016/j.xphs.2019.01.004.
157. Kiss, T.; Fenyvesi, F.; Pasztor, N.; et al. Cytotoxicity of Different Types of Methylated SS-Cyclodextrins and Ionic Derivatives. *Pharmazie* **2007**, 557–558, doi:10.1691/ph.2007.7.7051.
158. Rassu, G.; Fancello, S.; Roldo, M.; Malanga, M.; Szente, L.; Migheli, R.; Gavini, E.; Giunchedi, P. Investigation of Cytotoxicity and Cell Uptake of Cationic Beta-Cyclodextrins as Valid Tools in Nasal Delivery. *Pharmaceutics* **2020**, *12*, 658, doi:10.3390/pharmaceutics12070658.

ACKNOWLEDGEMENT

This work was supported by the Ministry of Human Capacities, Hungary grant TKP 2020 and 2.2.1-15-2016-00007 and GINOP-2.3.2-15-2016-00060 Projects.

NKFI OTKA K_146148 project and TKP2021-EGA-32 project with the support provided by the Ministry of Culture and Innovation of Hungary from the National Research, Development and Innovation Fund are also acknowledged.

I am also grateful for the support of ÚNKP-22-3-SZTE-163 and ÚNKP-23-3-SZTE-196 New National Excellence Programs provided by the Ministry for Culture and Innovation from the source of the National Research, Development and Innovation Fund.

I would like to express my gratitude to **Prof. Dr. Ildikó Csóka** for allowing me to carry out my Ph.D. studies in the Institute of Pharmaceutical Technology and Regulatory Affairs.

I am grateful for the guidance of my supervisors, **Prof. Dr. Rita Ambrus** and **Dr. Csilla Balla-Bartos** who contributed to raising the standards of my work with their valuable insights and advices. The work of my co-authors is also greatly appreciated, especially **Anett Motzwickler-Németh's**, who asked the right questions at the right times. Special thanks to the technicians of the Institute of Pharmaceutical Technology and Regulatory Affairs for their help. I would like to also highlight **Prof. Dr. Eva Roblegg**, who allowed me to join her research group for 3 months in Graz and provided insights into the mysteries of cell-culturing.

I am grateful for the friendships I have made and the opportunity to develop personally and professionally during my studies.

I greatly appreciate the emotional support of my **friends** and **family**, who were there for me the whole time and helped me through the lowest points.

Lastly, I would like to thank my **husband, Dr. Tamás Kiss** for his endless and unconditional love. I would not have been able to achieve the same things without his constant encouragement to step out of my comfort zone.